Unraveling 1,4-butanediol metabolism in *Pseudomonas putida* KT2440

Wing-Jin Li[1], Tanja Narancic[2,3], Shane T. Kenny[4], Paul-Joachim Niehoff[1], Kevin O'Connor[2,3], Lars M. Blank[1], Nick Wierckx[1,5]*

[1] Institute of Applied Microbiology-iAMB, Aachen Biology and Biotechnology-ABBt, RWTH Aachen University, Aachen, Germany

[2] UCD Earth Institute and School of Biomolecular and Biomedical Science, University College Dublin, Belfield, Dublin 4, Ireland

[3] BEACON – SFI Bioeconomy Research Centre, University College Dublin, Belfield, Dublin 4, Ireland

[4] Bioplastech Ltd., NovaUCD, Belfield Innovation Park, University College Dublin, Belfield, Dublin 4, Ireland

[5] Institute of Bio- and Geosciences IBG-1: Biotechnology, Forschungszentrum Jülich, 52425 Jülich, Germany

*** Correspondence:** n.wierckx@fz-juelich.de

Keywords: Laboratory Evolution, *Pseudomonas putida*, Proteomics, Genomics, Plastic upcycling

Abstract

Plastics, in all forms, are a ubiquitous cornerstone of modern civilization. Although humanity undoubtedly benefits from the versatility and durability of plastics, they also cause a tremendous burden for the environment. Bio-upcycling is a promising approach to reduce this burden, especially for polymers that are currently not amenable to mechanical recycling.

Wildtype *P. putida* KT2440 is able to grow on 1,4-butanediol as sole carbon source, but only very slowly. Adaptive laboratory evolution led to the isolation of several strains with significantly enhanced growth rate and yield. Genome re-sequencing and proteomic analysis were applied to characterize the genomic and metabolic basis of efficient 1,4-butanediol metabolism. Initially, 1,4-butanediol is oxidized to 4-hydroxybutyrate, in which the highly expressed dehydrogenase enzymes encoded within the PP_2674-2680 *ped* gene cluster play an essential role. The resulting 4-hydroxybutyrate can be metabolized through three possible pathways: i) oxidation to succinate, ii) CoA activation and subsequent oxidation to succinyl-CoA, and iii) beta oxidation to glycolyl-CoA and acetyl-CoA. The evolved strains were both mutated in a transcriptional regulator (PP_2046) of an operon encoding both beta-oxidation related genes and an alcohol dehydrogenase. When either the regulator or the alcohol dehydrogenase is deleted, no 1,4-butanediol uptake or growth could be detected. Using a reverse

engineering approach, PP_2046 was replaced by a synthetic promotor (14g) to overexpress the downstream operon (PP_2047-2051), thereby enhancing growth on 1,4-butanediol.

This work provides a deeper understanding of microbial 1,4-butanediol metabolism in *P. putida*, which is also expandable to other aliphatic alpha-omega diols. It enabled the more efficient metabolism of these diols, thereby enabling biotechnological valorization of plastic monomers in a bio-upcycling approach.

1 Introduction

Plastics, in all forms, are an ubiquitous cornerstone of modern civilization. They contribute greatly to a more efficient society, i.e., through the reduction of packaging weight, the increase in shelf life of foods, and the insulation of homes and refrigerators. Although humanity undoubtedly benefits from the versatility and durability of plastics, these characteristics also make them a tremendous burden for the environment. To reduce this impact, strategies beyond incineration, landfill and inefficient recycling are needed.

One of these approaches involves bio-upcycling, the microbial degradation of plastics and its conversion into value-added material (Wierckx et al., 2015; Narancic and O'Connor, 2017). Proofs of principle for the microbial conversion of selected plastics are already available. For instance, polyethyleneterephthalate (PET) was pyrolized and subsequently converted to polyhydroxyalkanoates (PHA) (Kenny et al., 2008; Kenny et al., 2012). A similar processes enabled conversion of polystyrene and polyethylene to PHA (Ward et al., 2006; Guzik et al., 2014). Polyurethanes (PU) are hardly amenable to mechanical recycling due to their molecular diversity and the fact that many PU are thermosets which can't be molten and re-molded. PU are produced by reacting aliphatic or aromatic diisocyanates with polyols and α,ω-diols as chain extenders. Depending on the monomer composition and chain lengths, polymer properties are diverse, which is key for PU's versatility. Applications can be found in paints and coatings, in building insulation and as sealants, as well as in flexible foams and absorbents for many end-user products like pillows and mattresses. In the context of a bio-upcycling strategy, bacteria and fungi have been found to degrade PU, including several Pseudomonads which grow on PU at high rates (Howard, 2002). A range of PU-degrading ester- and urethane hydrolases have been identified (Hung et al., 2016; Schmidt et al., 2017; Danso et al., 2019; Magnin et al., 2019b; Magnin et al., 2019a). Besides this, chemical recycling of PU is also possible with more mature technologies (Zia et al., 2007; Behrendt and Naber, 2009). In addition to the diamines, which are relatively valuable and can be extracted (Bednarz et al., 2017), typical PU monomers like adipic acid, 1,4-butanediol, and ethylene glycol are released during the process of depolymerization. Degradation pathways for ethylene glycol (Franden et al., 2018; Li et al., 2019) and adipic acid (Parke et al., 2001) are known. Yet, surprisingly little is known about the microbial catabolism of 1,4-butanediol.

1,4-butanediol is one of the major chain extenders used in the production of polyurethanes. It is also a common co-monomer in many polyesters such as polybutylene terephthalate and polybutylene adipate terephthalate. As commodity chemical, 1,4-butanediol is used to manufacture 2.5 million tons of plastics and polyesters (Yim et al., 2011). Additionally, it is used as a platform chemical to produce tetrahydrofuran and γ-butyrolactone, with a total market size valued at USD 6.19 billion in 2015 and is still growing (Grand View Research, 2017). So far, research was mainly focused on the sustainable production of 1,4-butanediol (Burgard et al., 2016). Its *de novo* microbial production was achieved in *E. coli* by identifying and implementing artificial routes for 1,4-butanediol biosynthesis (Yim et al., 2011). The verified and tested pathway starts with the TCA cycle intermediate succinyl-CoA. The heterologous CoA-dependent succinate semialdehyde dehydrogenase (SucD) from *Clostridium*

kluyveri and either a native or heterologous 4-hydroxybutyrate dehydrogenase from *C. kluyveri*, *Porphyromonas gingivalis* or *Ralstonia eutropha* catalyze the reaction from succinyl-CoA to 4-hydroxybutyrate. After CoA activation, 4-hydroxybutyryl-CoA will be further reduced by alcohol and aldehyde dehydrogenases to the final product 1,4-butanediol. In addition to this commonly used pathway, alternative potential routes via α-ketoglutarate, glutamate or acetyl-CoA were described (Yim et al., 2011). Conversion of xylose to 1,4-butanediol has also been described (Liu and Lu, 2015).

Butanol is a substrate with structural similarities to 1,4-butanediol. Usually, butanol concentrations above 1-2 % (135-270 mM) are toxic or at least growth-inhibiting for most of microbes, including *Pseudomonas putida* BIRD-1, DOT-T1E, and KT2440 (Cuenca et al., 2016). Nevertheless, *Pseudomonas* exhibits promising traits on tolerating, assimilating or at least surviving butanol (Rühl et al., 2009). To cope with butanol, classic solvent defense mechanisms like efflux pumps, membrane modifications or rebalancing of the redox state are activated (Ramos et al., 2002; Basler et al., 2018). . Further, *P. putida* KT2440 is capable of rapid butanol oxidation to butyrate via a variety of alcohol- and aldehyde dehydrogenases (Simon et al., 2015; Vallon et al., 2015; Cuenca et al., 2016). Prominent among these are PedE, PedH, and PedI alcohol and aldehyde dehydrogenases, encoded in the so-called ped cluster. These have a highly relaxed substrate specificity and are capable of oxidizing, among others, ethanol, phenylethanol, butanol, and butanal (butyraldehyde) (Wehrmann et al., 2017). The resulting butyrate is CoA-activated by acyl-CoA synthetases like AcsA1 (PP_4487), and subsequently undergoes β-oxidation.

Non-pathogenic Pseudomonads have an established track record in bioremediation and biodegradation processes (Samanta et al., 2002; Spini et al., 2018; Tahseen et al., 2019), and different strains of this genus are also suitable candidates to perform bio-upcycling (Kenny et al., 2008; Wierckx et al., 2015; Wilkes and Aristilde, 2017). One of the widely used biotechnological hosts is *P. putida* KT2440, which possesses extensive metabolic abilities (Nelson et al., 2002; Nikel et al., 2014; Nikel and Lorenzo, 2018). Being a soil bacterium and therefore exposed to different environmental surroundings, it is equipped with tolerances and metabolic capabilities towards a broad spectrum of substances. The 6.18 Mb genome of *P. putida* KT2440 harbours a broad spectrum of oxygenases, oxidoreductases as well as hydrolases, transferases, and dehydrogenases (Belda et al., 2016). This wide range of enzymes enables *P. putida* KT2440 to modify an abundance of alcohols and aldehydes (Wierckx et al., 2011).

In this work, *P. putida* KT2440 strains with an enhanced growth rate on 1,4-butanediol are obtained by adaptive laboratory evolution (ALE), and analyzed by proteomics and genome resequencing in order to determine possible degradation routes. The improved growth phenotype was subsequently reverse-engineered into the wildtype, thereby generating a deeper understanding of 1,4-butanediol metabolism, thereby broadening the applicability of *P. putida* for plastic upcycling.

2 Material and Methods

2.1 Chemicals, media and cultivation conditions

The chemicals used in this work were obtained from Carl Roth (Karlsruhe, Germany), Sigma-Aldrich (St. Louis, MO, USA), or Merck (Darmstadt, Germany) unless stated otherwise. Glycerol was kindly provided by Bioeton (Kyritz, Germany).

All strains used in this work are listed in **Table 1**. Cultivations were performed in LB – complex medium (10 g L^{-1} tryptone, 5 g L^{-1} yeast extract and 5 g L^{-1} sodium chloride) or, for quantitative microbiology experiments, in mineral salt medium (MSM) (Hartmans S. et al., 1989), solidified when

needed with 1.5 % agar (w/v), containing different amount of C source. Precultures were supplied with 20 mM glucose, whereas 20 mM 1,4-butanediol were used for studies with 1,4-butanediol.

Table 1 *Pseudomonas putida* strains used in this work with listed genotype and references.

no.	strain	genotype	reference
1	KT2440 wildtype	cured, restriction-deficient derivative of *P. putida* mt-2	Ramos-Díaz, 1998
2	B10.1	KT2440 ALE in BDO, single strain A6	this work
3	B10.2	KT2440 ALE in BDO, single strain C2	this work
4	KT2440 ΔPP_2046	ΔPP_2046 in KT2440	this work
	B10.1 ΔPP_2046	ΔPP_2046 in B10.1	this work
	B10.2 ΔPP_2046	ΔPP_2046 in B10.2	this work
5	KT2440 ΔPP_2046::14g	ΔPP_2046::14g in KT2440	this work
	B10.1 ΔPP_2046::14g	ΔPP_2046::14g in B10.1	this work
	B10.2 ΔPP_2046::14g	ΔPP_2046::14g in B10.2	this work
6	KT2440 Δ*ped*	Δ*pedE-I* in KT2440	Li et al., 2019
7	KT2440 Δ*pedE*	Δ*pedE* in KT2440	this work
	KT2440 Δ*pedH*	Δ*pedH* in KT2440	this work
8	KT2440 Δ*pedI*	Δ*pedI* in KT2440	this work
9	KT2440 ΔPP_2047-2051	knockout PP_2047-51 in KT2440	this work
	B10.A ΔPP_2047-2051	knockout PP_2047-51 in B10.A	this work
	B10.B ΔPP_2047-2051	knockout PP_2047-51 in B10.B	this work
10	KT2440 ΔPP_2049	ΔPP_2049 in KT2440	this work
	B10.1 ΔPP_2049	ΔPP_2049 in B10.1	this work
	B10.2 ΔPP_2049	ΔPP_2049 in B10.2	this work
11	KT2440 ΔPP_2051	ΔPP_2051 in KT2440	this work
	B10.1 ΔPP_2051	ΔPP_2051 in B10.1	this work
	B102 ΔPP_2051	ΔPP_2051 in B10.2	this work
	KT2440 ΔPP_0411-13	ΔPP_0411-13	this work
	B10.1 ΔPP_0411-13	ΔPP_0411-13	this work
	B10.2 ΔPP_0411-13	ΔPP_0411-13	this work

For plasmid maintenance, *E. coli* strains and *P. putida* KT2440 strains were cultivated in media supplemented with 50 mg L^{-1} kanamycin, which was sterilized by using a 0.2 µm syringe filter (Carl Roth GmbH + Co. KG, Karlsruhe, Germany).

Liquid cultivations were incubated at 30 °C for *Pseudomonas* and 37 °C for *E. coli*, 200 rpm shaking speed with an amplitude of 50 mm in a Multitron shaker (INFORS, Bottmingen, Switzerland) using 100 mL non-baffled Erlenmeyer flasks with metal caps, containing 10 mL culture volume for a pre-culture and 500 mL non-baffled Erlenmeyer flasks with metal caps, containing 50 mL culture volume for a main culture.

For online growth detection, 96-well plates with 200 µL or in 24-well plates with 4 – 3 mL culture volume were inoculated with a pre-culture containing 4 - 3 mL MSM with 20 mM glucose in 24-well System Duetz plates (Enzyscreen, Heemstede, The Netherlands), cultivated in a Multitron shaker (INFORS, Bottmingen, Switzerland) with a 300 rpm shaking speed with an amplitude of 50 mm. Inoculated Growth Profiler® plates were incubated at 30 °C, 225 rpm shaking speed with an amplitude of 50 mm in the Growth Profiler® 960 (Enzyscreen, Heemstede, The Netherlands).

Adaptive laboratory evolution (ALE) was performed as follows: a pre-culture of *P. putida* KT2440, cultivated in MSM with 20 mM glucose, was used to inoculate 250 mL clear glass Boston bottles with Mininert valves (Thermo Fisher Scientific, Waltham, MA, USA) containing 20 mM 1,4-butanediol for the adaptation on 1,4-butanediol (final OD_{600} of 0.01). Serial transfers were reinoculated several times after the cultures reached an OD_{600} of at least 0.5, with a starting OD_{600} of 0.1. After growth was detected (usually overnight), single colonies were isolated from ALE cultures by streaking samples on LB agar plates. After ALE on 1,4-butanediol, two strains (B10.1 and B10.2) out of 72 strains were selected according to their growth behavior in MSM with 20 mM 1,4-butanediol determined using the Growth Profiler® 960 (Enzyscreen, Heemstede, The Netherlands).

Growth experiments for PHA accumulation were carried out in 250 ml Erlenmeyer flasks containing 50 ml of nitrogen limited MSM medium supplemented with 80 mM 1,4 butanediol. Nitrogen limited MSM medium contains 9g/L $Na_2HPO_4.12H_20$, 1.5g/L KH_2PO_4, 0.25 g/l NH_4Cl, trace elements. An overnight culture was prepared by inoculating 2 ml of medium with a single colony from a plate and incubating overnight at 30°C and shaking at 200 rpm. 500 µl of the 2 ml MSM overnight culture was used as an inoculum for the 50 ml cultures which were incubated under the same conditions for 48 h. Octanoic acid (20 mM) was added to some flasks after 24 hours.

2.2 Molecular work

2.2.1 DNA procedures

The construction of plasmids was performed either by standard restriction-ligation or Gibson assembly (Gibson et al., 2009) using the NEBuilder HiFi DNA Assembly (New England Biolabs, Ipswich, MA, USA). DNA modifying enzymes were purchased from New England Biolabs, for dephosphorylation Fast AP Thermo Sensitive Alkaline Phosphatase (ThermoScientific, Langenselbold, Germany) was used. Primers were purchased as unmodified DNA oligonucleotides from Eurofins Genomics (Ebersberg, Germany) and are listed in Table S 1. Clonal DNA sequences were amplified using the Q5 High-Fidelity Polymerase (New England Biolabs, Ipswich, MA, USA). DNA- ligations were performed by using T4 ligase from Fermentas (ThermoScientific, Langenselbold, Germany) according to the protocol. Arbitrary-primed PCR was performed as described by Martínez-García et al. (2014). For the transformation of DNA assemblies and purified plasmids (Table S 2) into competent *E. coli* a heat shock protocol was performed (Hanahan, 1983). For *P. putida* transformations either conjugational transfer or electroporation were performed as described by Wynands et al. (2018). Knockout strains were obtained using the pEMG system described by Martínez-García and Lorenzo (2011) with a modified protocol described by Wynands et al. (2018). Plasmid inserts and gene deletions were confirmed by Sanger sequencing performed by Eurofins Genomics (Ebersberg, Germany).

In order to perform PCR directly from bacteria the alkaline polyethylene glycerol-based method was used (Chomczynski and Rymaszewski, 2006). Therefore, cell material was picked and dissolved in 50 µL of the reagent, containing 60 g PEG 200 with 0.93 mL 2 M KOH and 39 mL water, with a pH of 13.4. After incubation for 3-15 min, 2 µL of the sample was used as template in a 25 µL PCR reaction.

2.3 Analytical methods

2.3.1 Growth monitoring methods

Bacterial growth was monitored as optical density at a wavelength of λ = 600 nm (OD_{600}) with an Ultrospec 10 Cell Density Meter (GE Healthcare, Little Chalfont, Buckinghamshire, UK). Growth rates (µ) are determined by fitting an exponential curve to a plot of OD_{600} over time of a culture in the exponential phase. This is now mentioned in the materials and methods section. The online analysis of growth using the Growth Profiler® was analyzed using the Growth Profiler® Control software V2_0_0. Cell densities are expressed as G-value, which is derived from imaging analysis of microtiter plates with transparent bottoms.

2.3.2 PHA analysis

Cells were harvested by centrifugation at 3320xg for 10 minutes and then lyophilized and weighed for determination of cell dry weight. PHA content was determined by subjecting lyophilized cells to acidic methanolysis (Brandl et al., 1988; Lageveen et al., 1988). 5 - 10 mg of dried cells were resuspended in 2 ml of acidified methanol (15 % H_2SO_4, v/v) and 2 ml of chloroform containing 6 mg/l benzoate methyl ester as an internal standard. The solution was placed in 15 ml Pyrex test tubes, sealed and incubated at 100°C for 3 hours. The tubes were then placed on ice for 1 min. 1 ml of water was added to each tube and the solution mixed by vigorous vortexing. The phases were allowed to separate, and the organic phase was removed and passed through a filter before further analysis.

The 3-hydroxyalkanoic acid methyl esters were analyzed by gas chromatography (GC) using an Agilent 6890N chromatograph equipped with a HP Innowax column (30 m x 0.25 mm x 0.5 µm) and a flame ionization detector (FID). An oven ramp cycle was employed as follows, 120°C for 5 min, increasing by 3°C/min to 180°C, 180°C for 10 min. A 20:1 split was used with helium as the carrier gas and an inlet temperature of 250 ˚C. Commercially available 3-hydroxyalkanoic acids (Bioplastech Ltd Dublin Ireland) were methylated as described above for PHA samples and used as standards to identify PHA monomers.

2.3.3 Extracellular metabolites

For measuring extracellular metabolites, samples taken from liquid cultivation were centrifuged for 3 min at 17,000×g to obtain supernatant for High-Performance Liquid Chromatography (HLPC) analysis using a Beckman System Gold 126 Solvent Module equipped with a Smartline 2300 refractive index detector (Knauer, Berlin, Germany). Analytes were eluted using a 300 x 8 mm organic acid resin column together with a 40 x 8 mm organic acid resin precolumn (both from CS Chromatographie, Langerwehe, Germany) with 5 mM H_2SO_4 as mobile phase at a flow rate of 0.7 ml min^{-1} at 70 °C. (Li et al., 2019).

2.3.4 **Genome sequencing**

Genomic DNA for resequencing was isolated through a High Pure PCR Template Preparation Kit (ROCHE life science, Basel, Switzerland). Sequencing and SNP/InDel (single nucleotide polymorphism/ insertion and deletion polymorphism) calling was done by GATC (Konstanz, Germany) using Illumina technology as paired-end reads of 125 base pairs. To map the reference sequence against the database, BWA with default parameters was used (Li and Durbin, 2009). SNPs and InDels, analyzed by GATK´s UnifiedGenotyper (McKenna et al., 2010; DePristo et al., 2011), were listed and visualized with the Integrative Genomics Viewer (IGV) (Thorvaldsdóttir et al., 2013).

The sequences have been deposited in the NCBI Sequence Read Archive (SRA) with the accession number SRP148839 for ethylene glycol ALE strains (including our laboratory wildtype SRX4119395 used in this study) and SRP148839 for the 1,4-butanediol ALE strains.

2.3.5 **Proteomics**

The evolved strains B10.1 and B10.2 were cultivated along with the wild type *P. putida* KT2440 in 50 ml MSM medium supplemented with 20 mM 1,4-butanediol or 13 mM glucose (both equivalent to 80 mM C). The cultures were harvested by centrifugation and prepared for proteomic analysis as previously described (Narancic et al., 2016). Samples were sent to T. Narancic at University of Dublin to perform the following protocol. For total protein concentrations, peptide fragments obtained by trypsin digestion were analyzed on the Q-Exactive Hybrid Quadrupole Orbitrap Mass Spectrometer (MS; Thermo Scientific) connected to a Dionex Ultimate 3000 (RSLCnano; Thermo Scientific) chromatography system (Buffer A: 97 % water, 2.5 % acetonitrile, 0.5 % acetic acid; buffer B: 97 % acetonitrile, 2.5 % water, 0.5 % acetic acid; all solvents were LC-MS grade). The mass spectrometer was operated in positive ion mode with a capillary temperature of 320 °C and a potential of 2300 V applied to the frit. All data were acquired with the MS operating in automatic data-dependent switching mode. A high-resolution (70,000) MS scan (300–1600 m/z) was performed using the Q Exactive to select the 12 most intense ions prior to MS/MS analysis using HCD. The identification and quantification were performed using the Andromeda peptide identification algorithm integrated into MaxQuant (Cox and Mann, 2008; Cox et al., 2011). *P. putida* KT2440 protein sequence database downloaded from UniProt (www.uniprot.org) in April 2016 was used as a reference (The UniProt Consortium, 2019). Label-free quantification (LFQ) was used to compare the expression level of proteins across samples and growth conditions (Wang et al., 2003). Proteins with a 2-fold change or higher and a significant change in t-test (FDR 0.01) were automatically accepted, while spectra with no specific change were manually checked for quality.

Each sample had three biological replicates, and each biological replicate was then prepared for the proteomic analysis as a technical replicate. Statistical analysis was performed using Perseus and built-in Welche's t-test with FDR set at 0.01 (Tyanova et al., 2016b). The proteins with at least 2-fold change were functionally annotated using David bioinformatics (Huang et al., 2009a, 2009b) and clustered into orthologous groups using EggNOG (Huerta-Cepas et al., 2016).

2.3.6 **Detection of dehydrogenase activity**

To perform the enzyme assay, cells from a pre-culture were used to inoculate the main culture containing 20 mM glucose and 5 mM 1,4-butanediol. After 16 h of cultivation, crude extract was isolated using BugBuster (Merck, Darmstadt, Germany) and was desalted using PD-desalting columns (GE Healthcare, Buckinghamshire, UK) and eluted in 100 mM glycinglycin buffer. Protein

concentrations were estimated by standard Bradford test at 595 nm. For the dehydrogenase assay, a modified protocol from Kagi and Vallee B. H. (1960) was followed, in which 5 mM 4-hydroxybutyrate or 4 % ethanol as control were used as substrate. The formation of NADH was measured at 340 nm in a 96-well-plate at 30 °C in a well plate reader from Synergy Mx from Biotek (Bad Friedrichshall, Germany). To obtain a homogeneous mixture, after the addition of NAD^+ or 4-hydroxybutyrate, the well-plate was shaken for three seconds at highest speed available.

2.3.7 Statistics

Statistical probability values were, if not stated otherwise, calculated using a paired Student's t-distribution test with homogeneity of variance (n = 3, significance level of 0.05). In case of duplicates, errors are expressed as deviation from the mean (n = 2).

3 Results

3.1 Isolation of strain with enhanced growth on 1,4-butanediol by ALE

To study the growth of *P. putida* KT2440 and possible intermediate production when metabolizing 1,4-butanediol, growth experiments in shake flasks were performed. The wildtype showed poor growth (μ_{max} = 0.082 ± 0.004 h^{-1}) on MSM with 20 mM 1,4-butanediol, requiring more than 50 h to consume all substrate (t = 49; 1.3 ± 0.1 mM), while secreting high levels of the oxidation product 4-hydroxybutyrate (t = 49 h; 16.8 ± 0.3 mM). (**Figure 1**). This slow growth implies that in principle the metabolic routes are present in *P. putida* KT2440, but they are not operating optimally under the chosen conditions.

To enhance its ability to grow on 1,4-butanediol, wildtype *P. putida* KT2440 was subjected to adaptive laboratory evolution (ALE). This method is known to enable the selection of mutated strains with enhanced properties towards specific environments, likely affecting transcriptional regulatory systems (Dragosits and Mattanovich, 2013; Lennen et al., 2019; Li et al., 2019). Cultures of *P. putida* KT2440 were serially re-inoculated to fresh media containing 20 mM 1,4-butanediol ten times, as soon as growth was observed in form of optical densities above 0.8 (**Figure 1**). All three parallel evolution lines grew with the same trend. While the first three batches reached an OD_{600} between 0.8 and 2 after 3-4 days, later batches reached an OD_{600} between 2.5 and 3.5 after two days or less. The ALE was stopped after approximately 47 generations, when growth on 1,4-butanediol reached an OD_{600} of 2.5 overnight. Single colonies were isolated by streaking the three ALE cultures on LB plates. From each of the three evolution lines, 24 single colonies were tested for growth on 1,4-butanediol in a 96- well plate using a Growth Profiler® (**Figure 1**). Overall, the growth of these single clones was relatively similar, indicating a rather homogeneous evolved population. The two strains with the highest growth rates were selected, from different evolutionary lines, according to their growth in MSM with 20 mM 1,4-butanediol. These isolated clonal strains are named B10.1 and B10.2 (**Figure 1**).

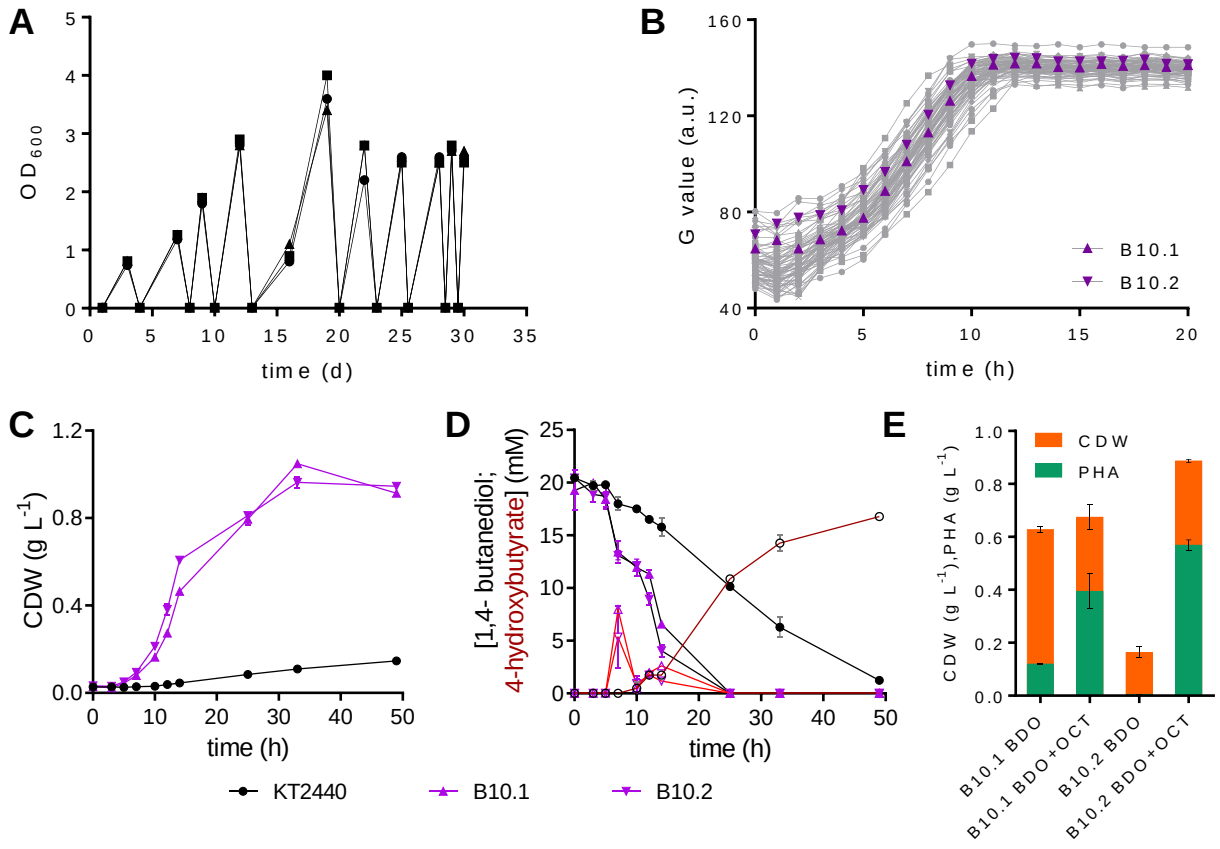

Figure 1 Adaptive laboratory evolution of *P. putida* KT2440 on 1,4-butanediol. **A)**: Three parallel lines sequential batch cultivations on MSM with 20 mM 1,4-butanediol. **B**) Growth of single strains isolated from each ALE batch on MSM with 20 mM 1,4-butanediol. The strains B10.1 (purple triangle) and B10.2 (purple inverted triangle) were selected for further investigation. Growth was detected via a Growth Profiler® using a 96-well plate. **C**) Biomass growth and **D**) 1,4-butanediol (closed symbols, black lines) and 4-hydroxybutyrate (open symbols, red lines) measured in cultures of the wildtype and evolved strains B10.1 and B10.2 in MSM with 20 mM 1,4-butanediol. **E)** Growth and PHA formation of strains B10.1 and B10.2 cultivated for 48 h in nitrogen-limited MSM medium with 80 mM 1,4-butanediol (BDO), supplemented with or without 20 mM octanoic acid (OCT) after 24 h. Cultures took place in 250 ml Erlenmeyer shake flasks with a culture volume of 50 ml. Error bars indicate the deviation of the mean (n = 2).

The two evolved strains grew faster on 1,4-butanediol than the wildtype, even after several generations in complex medium or MSM containing glucose, indicating that the observed phenotype was evolutionary fixed in the genome. The single evolved isolates B10.1 and B10.2 reach growth rates of $0.33 \pm 0.054\ h^{-1}$ and $0.31 \pm 0.001\ h^{-1}$, respectively. In contrast to the wildtype they completely consume all carbon source, reaching maximum biomass concentrations of $1.05 \pm 0.0\ g_{cdw}\ L^{-1}$ and $0.96 \pm 0.02\ g_{cdw}\ L^{-1}$ after 33 h. This translates to an average biomass yield of 0.56 ± 0.025 g/g for the evolved strains. This relatively high yield is likely caused by the high degree of reduction of butanediol, providing considerable reducing equivalents especially in the initial oxidation reactions (Li et al., 2019). In contrast to the wildtype, the evolved strains only transiently accumulate low concentrations of 4-hydroxybutyrate, which are rapidly metabolized within four hours (**Figure 1**). All 1,4-butanediol and derivatives that could be detected by HPLC were consumed within 25 h, although biomass still increased significantly beyond this point. Other intermediates not detected by HPLC, possibly the

lactone of 4-hydroxybutyrate, could likely accumulate transiently in the cultures of the evolved strains. However, the high biomass yield suggests that all carbon source was consumed at the end of the culture.

In order to assess the applicability of these evolved strains in a bio-upcycling approach, they were cultured in a nitrogen-limited MSM medium with 80 mM 1,4-butanediol. Further cultures were supplemented with 20 mM octanoic acid after 24 hours. These conditions enable the production of polyhydroxyalkanoate (PHA) from a (co-)feed of 1,4-butanediol. Without octanoic acid co-feed, strain B10.1 strains reached a final biomass concentration of 0.63 ± 0.11 g L^{-1}, of which 19% (0.12 ± 0.003 g L^{-1}) is PHA. Surprisingly, strain B10.2 reached a much lower biomass density, with only 3% PHA. With an octanoic acid co-feed, strain B10.2 reached the highest biomass concentrations of 0.89 ± 0.005 g L^{-1}, of which 64% (0.57 ± 0.02 g L^{-1}) is PHA (**Figure 1**). This proves that 1,4-butanediol can be used as a (co-)substrate for the production of a value-added biopolymer, thereby in principle enabling the upcycling of e.g. hydrolyzed PU or polyester waste.

Evolution successfully yielded strains with a 4- or 3.7-fold improved growth rate on 1,4-butanediol compared to the wildtype. The fact that the wildtype accumulates much more 4-hydroxybutyrate than the evolved strains indicates that this is likely the main metabolic bottleneck which was affected by ALE.

3.2 Systems analysis of 1,4-butanediol degradation in *P. putida* KT2440

To investigate the molecular basis of their enhanced growth on 1,4-butanediol, the genomes of the evolved strains B10.1 and B10.2 were resequenced (NCBI SRA accession number SRP148839). The sequences were compared to our laboratory wildtype (SRX4119395) and a reference database genome of *P. putida* KT2440 (Belda et al., 2016, AE015451.2). A comparison of the latter two was previously described in the context of ethylene glycol metabolism in *P. putida* (Li et al., 2019). Therefore, we focus here only on differences between our laboratory wildtype and the B10 strains. In the evolved strains B10.1 and B10.2, seven and eight mutations, respectively, were identified in addition to the mutations already present in the laboratory wildtype. Most of these mutations were either silent or intergenic. In addition to these, in the genome of B10.1, an in-frame deletion of 69 bp was found in PP_2139, encoding DNA topoisomerase I. Since this enzyme is related to DNA replication and repair (Wang, 2002), this alteration is unlikely to affect 1,4-butanediol metabolism specifically. However, this mutation might still be favorable in a general sense by affecting growth rate through DNA replication. Furthermore, a missense mutation was identified B10.2 that affects PP_2889, encoding the transmembrane anti-sigma factor PrtR (Calero et al., 2018) (**Table S3**). An amino exchange (A240G, GCG/GGG) in this regulator, involved in temperature-related protease production (Burger et al., 2000), might enhance tolerance towards 1,4-butanediol and its oxidation products. Both of these mutations are likely related to general ALE effects selecting for faster growth or higher tolerance to chemical stressors, rather than affecting the operation of the metabolic network.

The PP_2046 gene, encoding for a LysR-type transcriptional regulator, stood out for being mutated in both evolved strains, with each carrying a different mutation. In B10.1, a nonsense mutation caused the loss of the start codon (ATG/ATA), while in B10.2 a missense mutation caused an amino acid exchange (E34G, GAG/ GGG) in the helix-turn-helix DNA binding domain of the regulator (**Figure S1, Table S3**). The mutations in this regulator likely affect the expression of the adjacent operon PP_2047-51 which encodes an iron-containing alcohol dehydrogenase, as well as enzymes involved in β-oxidation (Li et al., 2019).

In addition to the analysis of the changes on the genome level, proteomic analysis of the evolved strains and the wildtype during growth on glucose and 1,4-butanediol was conducted. This was done to

identify relevant enzymes that are either constitutively expressed or natively induced by 1,4-butanediol. Three biological samples from each strain and culture condition, either grown on glucose or 1,4-butanediol in MSM, were harvested at mid-log phase (**Figure S2**). The samples were normalized using total protein concentration to give the same starting protein concentration for all replicates.

In total, 2122 proteins were identified across all samples and growth conditions, representing 40% of the *P. putida* KT2440 proteome. The identified proteins exhibited a wide range of annotated biophysical (molecular mass, isoelectric point), biochemical (functional annotations) and structural (domains) properties, suggesting that the analysis was not biased in favour of, or against, any protein class.

When cultivated on 1,4-butanediol the evolved strain B10.1 expressed 19 proteins which were not present in the wildtype, while 313 proteins were up- or downregulated at least two-fold compared to the wildtype. When evolved strain B10.2 was compared to the wildtype, 138 proteins showed at least two-fold difference in expression. The two evolved strains differed in their expression of 126 proteins. A large fraction of the differentially expressed proteins have no known function (**Figure 2**, **Supplemental data file 2**). The second-largest group can be categorized in amino acid metabolism and transport according to the clusters of orthologous groups (COG) classification (Tatusov et al., 1997). The likely reason for this large number of proteins with different expression levels is a large difference in growth rate of the B10 strains and the wildtype on 1,4-butanediol and the turnover of proteins during growth.

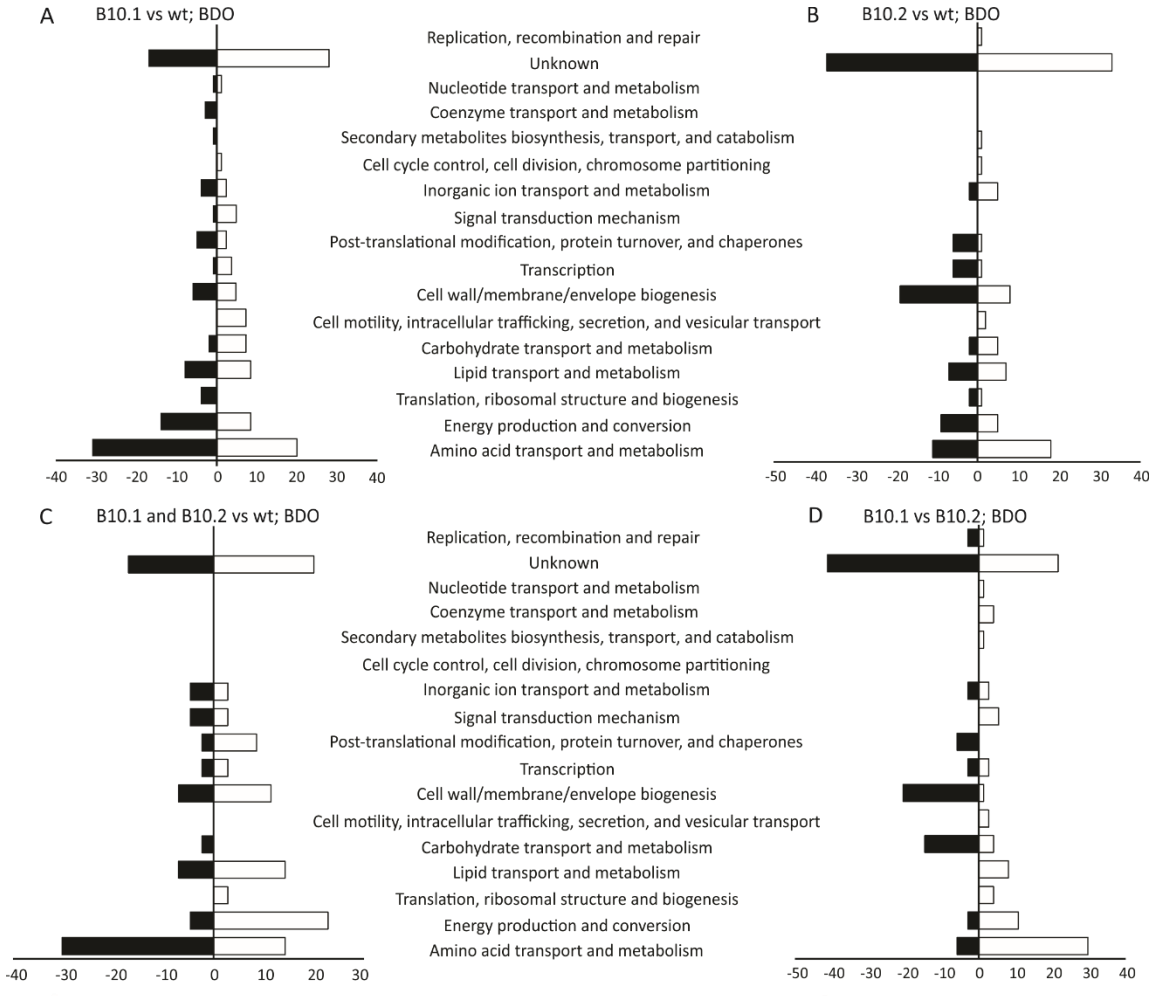

Figure 2 Proteins with significantly different levels of expression between the evolved strain B10.1 and wildtype *P. putida* KT2440 (**A**), the evolved strain B10.2 and wildtype *P. putida* KT2440 (**B**), the proteins showing the same trend of upregulation or downregulation in both evolved strains compared to the wild type (**C**), and the proteins with different levels of expression in B10.1 and B10.2 (**D**) when grown with 1,4-butanediol (BDO) as a carbon and energy substrate. The number of proteins showing ≥2-fold change (T test, FDR 0.01) in expression are given as clusters of orthologous groups (COG).

The top three highest expressed proteins during growth on glucose as well as 1,4-butanediol were PedE (ethanol dehydrogenase - PP_2674), PedI (aldehyde dehydrogenase - PP_2680) and Tu-B (PP_0452), an elongation factor which is involved in the regulation of protein synthesis by mediating aminoacyl tRNA into a free site of ribosomes (Noel and Whitford, 2016). The latter Tu-B is a general growth-associated protein (Klumpp et al., 2009). The former two proteins are encoded within the ped cluster (PP_2663-80) (Li et al., 2019). To focus on 1,4-butanediol metabolism, specific proteins with activities in putative catabolic pathways (**Figure 3**) and associated transport steps were focused on.

Genome sequencing uncovered mutations in PP_2046. The corresponding protein was not detected in the proteome analysis, indicating no or a low basal expression below the detection limit of the applied method, which is not uncommon for transcriptional regulators. Proteins encoded by the downstream β-oxidation-related operon were strongly upregulated in the wildtype grown on 1,4-butanediol vs. glucose, including a 3-hydroxyacyl-CoA dehydrogenase (PP_2047, 22-fold), an acyl-CoA dehydrogenase (PP_2048, 16-fold), an iron-containing alcohol dehydrogenase (PP_2049, 52-fold), and an acetyl-CoA acetyltransferase (PP_2051, 25-fold). The hypothetical protein PP_2050 was not detected. On top of this strong induction by 1,4-butanediol in the wildtype, the genes in this operon were even further induced by 2.4- to 3-fold in the evolved strains compared to the wildtype (**Figure 3**, **Supplemental data file 2**).

Theoretically, 1,4-butanediol can be metabolized through three possible pathways, all branching off at the point of 4-hydroxybutyrate. This 4-hydroxybutyrate was rapidly formed in cultivations of wildtype *P. putida* KT2440 on 1,4-butanediol, and also accumulates transiently with the B10 strains (**Figure 1**). This shows that oxidation of 1,4-butanediol to 4-hydroxybutyrate via alcohol and aldehyde oxidases already occurs at a high rate in the wildtype. The high expression levels of PedE, PedH and PedI suggest that these enzymes are major players in these oxidation steps. Although the encoding genes were not affected by the ALE, and they are only marginally upregulated when the strains were grown with 1,4-butanediol in comparison with growth on glucose, they are constitutively expressed on a very high level. This indicates a considerable metabolic investment of *P. putida* to be prepared for alcohol and aldehyde oxidation. This rapid oxidation is especially important for tolerance against the highly toxic aldehydes (Franden et al. 2018). Apparently, *P. putida* encounters such aldehydes often enough in its native environment to warrant this high constitutive expression. Besides these two enzymes, a number of other oxidoreductases are strongly induced upon growth on 1,4-butanediol vs. glucose. These include the GMC family oxidoreductase PP_0056 (BetA-I, along with its associated transporter PP_0057), the iron-containing alcohol dehydrogenase PP_2049, the 3-hydroxybutyrate dehydrogenase PP_3073 (HbdH), the isoquinoline oxidoreductase PP_3621-3 (IorAB-adhB), and the aldehyde dehydrogenase PP_5258 (amaB).

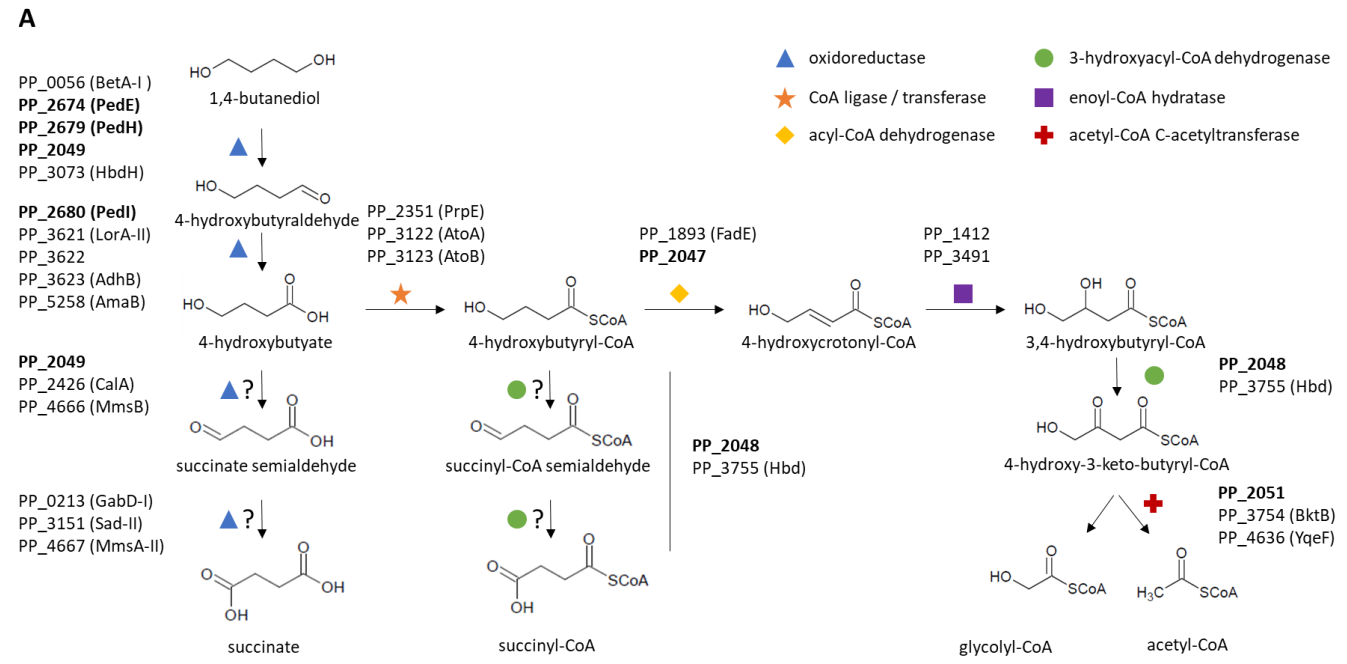

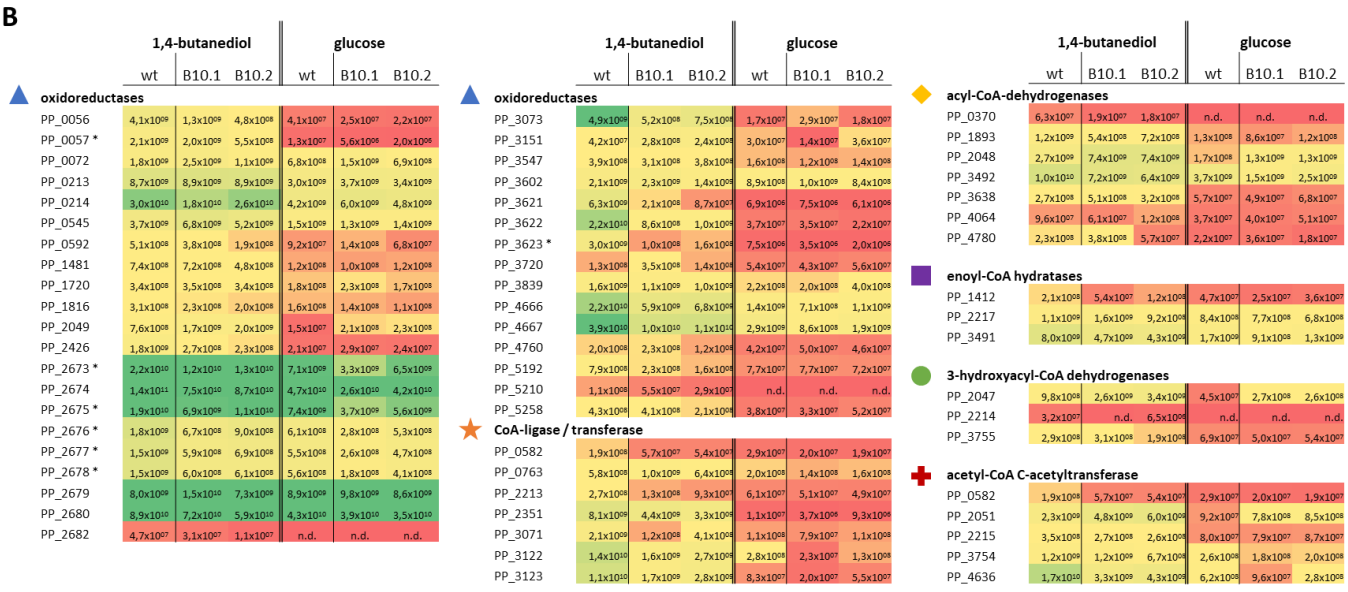

Figure 3 Hypothetical pathways for 1,4-butanediol metabolism (**A**) and expression levels (Label Free Quantification, LFQ (Tyanova et al., 2016a)) representing the sum of the ion signal recorded in the mass spectrometer for all peptides derived from each protein of the corresponding proteins (**B**). Colors correspond to LFQ levels, red for low, yellow for average, and green for high values. Proteins which are strongly upregulated in response to growth on MSM with 1,4-butanediol compared to growth with glucose, or which have high expression level in all tested conditions, are indicated in **A**, with proteins further investigated in this work in bold. Protein expression levels of selected proteins for *P. putida* KT2440 and the evolved strains B10.1 and B10.2 growing in MSM with glucose or 1,4-butanediol are listed as oxidoreductases (blue triangle), CoA-ligases (orange star), acyl-CoA dehydrogenases (yellow diamond), 3-hydroxyacyl-CoA dehydrogenase (green circle), enoyl-CoA hydratases (purple rectangle) and acetyl-CoA C-actyltransferase (red cross). n/d= not detected. In case of operons, associated transporters or accessory proteins are included, marked with *.

Also of note was the relatively strong differential expression of genes related to the metabolism and transport of amines. The PP_0411-4 operon was highly expressed in the wildtype, but not in the evolved strains, during growth on 1,4-butanediol (Supplemental data file 2). This operon encodes a polyamine ABC transporter for spermidine and putrescine, which are structurally and chemically similar to 1,4-butanediol. In spite of this large differential expression, no genomic mutations were found in the evolved strains surrounding the operon, and the knockout of PP_0411-14 in *P. putida* KT2440 did not influence growth on 1,4-butanediol (data not shown). In contrast, operons encoding metabolic pathways for 4-aminobutanoate (PP_2013-15), ethanolamine (PP_0542-44), and ornithine (PP_0999-1001) were strongly upregulated on 1,4-butanediol vs. glucose (**Supplemental data file 2)**. The metabolism of some of these amines shares metabolic intermediates with the putative 1,4-butanediol pathways (Bandounas et al., 2011). Possibly, the high accumulation of 4-hydroxybutyrate in the wildtype induced the expression of this transporter, leading to a misregulation during growth on 1,4-butanediol. Alternatively, one of the aldehyde intermediates may undergo amination, or the diamine transporter may facilitate uptake of 1,4-butanediol or its oxidation products.

3.3 Pathway validation

The abovementioned genomic and proteomic analyses indicate several possible genes and enzymes that are either natively expressed at a high level, upregulated in the presence of 1,4-butanediol, or activated by ALE. To test the relevance of these genes for 1,4-butanediol metabolism, several knockout strains were generated. The dehydrogenases encoded in the ped cluster (PP_2673-80) were constitutively expressed at a high level (**Figure 3**). To test the importance of these dehydrogenases to the degradation of 1,4-butanediol, the entire cluster (Δ*pedE-I*), as well as individual genes *pedE* and *pedI*, were knocked out in *P. putida* KT2440. When *P. putida* KT2440 Δ*pedE-I* was cultivated in MSM with 1,4-butanediol no growth could be observed, nor was the substrate taken up or converted to 4-hydroxybutyrate (**Figure 4**). Therefore, this cluster appears to be essential for the uptake and metabolism of 1,4-butanediol. The fact that no oxidation products were observed strongly suggests that these enzymes catalyze the initial oxidation steps.

The single knockouts of *pedE* and *pedI* were streaked on MSM plates containing 20 mM 1,4-butanediol as sole carbon source. Of these knockouts, *P. putida* KT2440 Δ*pedE* did not grow, while the Δ*pedI* strain displayed growth similar to the wildtype after 48 h (**Figure 4**). Thus, the PQQ-dependent alcohol dehydrogenase PedE is likely responsible for the oxidation of 1,4-butanediol, while, surprisingly, the aldehyde dehydrogenase PedI does not seem to play an essential role in the further oxidation steps, likely because of the high redundancy of aldehyde dehydrogenases in *P. putida*. PedE, a homolog to ExaA from *P. aeruginosa*, is an extensively investigated pyrroloquinoline quinone alcohol dehydrogenase with a broad substrate activity, including 1-butanol and 1,4-butanediol (Takeda et al., 2013). Furthermore, Wehrman *et al.* (2017) showed activities of PedE towards structural similar alcohols and aldehydes of 1,4-butanediol, like 1-butanol and butyraldehyde. Additionally, the first steps of 1-butanol assimilation in *P. putida* BIRD-1 also involve homologs of the *ped* cluster (Simon et al., 2015; Vallon et al., 2015; Cuenca et al., 2016). The other dehydrogenases encoded within the *ped* cluster, PedH and also PedI, seem to be of minor relevance. PedE and PedH are both ethanol dehydrogenases but are inversely regulated by lanthanides. In the absent of those rare earth elements, *pedE* expression is induced and *pedH* is repressed (Wehrmann et al., 2017). Both PedE and PedH are highly expressed, but considering the absence of lanthanides, it is likely that PedH is not active.

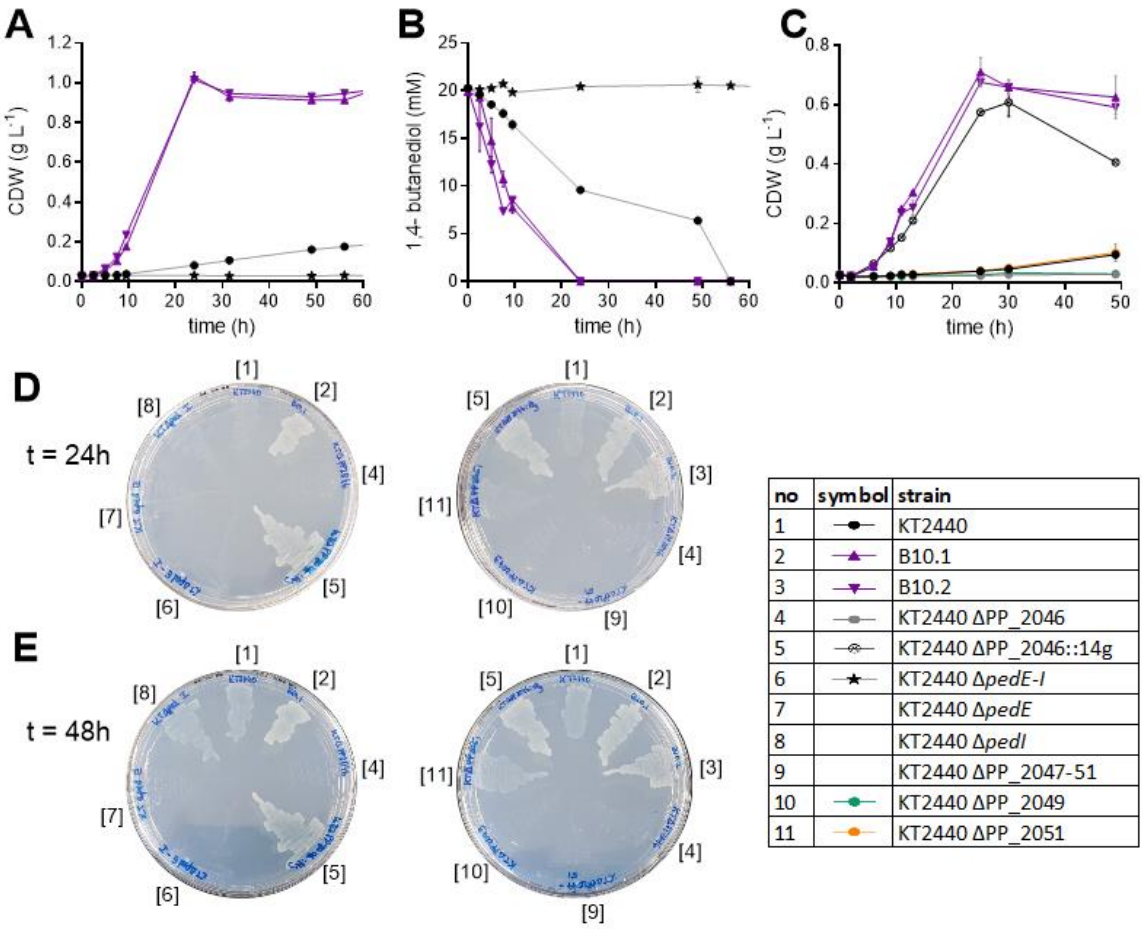

no	symbol	strain
1		KT2440
2		B10.1
3		B10.2
4		KT2440 ΔPP_2046
5		KT2440 ΔPP_2046::14g
6		KT2440 Δ*pedE-I*
7		KT2440 Δ*pedE*
8		KT2440 Δ*pedI*
9		KT2440 ΔPP_2047-51
10		KT2440 ΔPP_2049
11		KT2440 ΔPP_2051

Figure 4 Analysis of knockout strains of *P. putida* KT2440. Biomass growth (**A**) and 1,4-butanediol concentrations (**B**) of the wildtype, evolved strains and the Δ*pedE-I* knockout cultivated in shake flasks in MSM with 20 mM 1,4-butanediol. Growth of selected strains on 20 mM 4-hydroxybutyrate (**C**). Growth of selected strains on MSM agar plates with 20 mM 1,4-butanediol after 24 h (**D**) and 48 h (**E**). Strain numbers next to the plates correspond to full strain names listed in Table 1. The contrast of the images was increased by 20% to improve visibility. Error bars indicate the deviation of the mean (n = 2).

The mutations found in PP_2046 and the upregulation of the adjacent operon PP_2047-51 strongly indicates an important role of the encoded enzymes. This operon contains an iron-containing alcohol dehydrogenase encoded by PP_2049 in addition to β-oxidation related genes. In literature, this dehydrogenase is placed in a context of β-oxidation, likely due to its association with the other genes in the PP_2047-51 operon (Poblete-Castro et al., 2012). However, PP_2049 is classified as an iron-containing alcohol dehydrogenase, which belongs to type III non-homologous NAD(P)$^+$-dependent alcohol dehydrogenases (Mitchell et al., 2019). This family is known to have activity towards methanol, ethanol, propanol and butanol (Hiu et al., 1987; Gaona-López et al., 2016). It is highly likely that PP_2049 oxidizes one or more of the alcohol groups of 1,4-butanediol. Thus, neither direct oxidation to succinate nor β-oxidation can be ruled out by the observed mutation in PP_2046 and the upregulation of the associated operon. In order to determine the relevance of the operon and to distinguish between the effect of the alcohol dehydrogenase and the β-oxidation related genes, the operon and individual genes PP_2046, PP_2049, and PP_2051 were knocked out in wildtype *P. putida*

KT2440 and in the evolved strains B10.1 and B10.2. Care was taken to avoid polar effects in the in-operon knockouts by leaving start and stop codons of overlapping genes intact using the pEMG system (Martínez-García and Lorenzo, 2011). Deletion strains were tested for their ability to grow on MSM with 1,4-butanediol or 4-hydroxybutyrate as sole carbon source (**Figure 4**).

Both the wildtype and the evolved strains were unable to grow on 1,4-butanediol or 4-hydroxybutyrate when the regulator PP_2046, or the alcohol dehydrogenase PP_2049 were deleted (**Figure 4**, **Figure 5**). The knockout of the whole operon also abolished growth. In contrast, deletion of PP_2051 did not affect growth on 1,4-butanediol **(Figure S3)**. This strongly suggests that PP_2049 is the main enzyme involved in the oxidation of 4-hydroxybutyrate. Both individual knockout strains of PP_2049 and *pedE* were unable to grow on 1,4-butanediol, making it unlikely that they oxidize the same substrate. More likely, the PP_2049 dehydrogenase is essential for the oxidation of 4-hydroxybutyrate, while PedE oxidizes 1,4-butanediol. Attempts to obtain direct biochemical evidence for the oxidation hypothesis with dehydrogenase assays on whole cell extracts of *P. putida* KT2440 wildtype, B10.1, and ΔPP_2046 with 4-hydroxybutyrate as a substrate were unsuccessful (**Figure S4**) although this might be caused by instability of the PP_2049 enzyme and should be investigated further. The lack of phenotype of the PP_2051 mutant suggests that β-oxidation is not involved, however, this is no clear proof since several other acetyl-CoA C-acetyltransferases are also expressed on a similar level (**Figure 3**).

The deletion of PP_2046 apparently causes a downregulation of the operon, while the mutations in PP_2046 in the evolved strains cause an overexpression of the adjacent operon. This is evident in the proteome data and also described in Li et al. (2019) for the E34G mutation in the context of ethylene glycol metabolism. In fact, the strains evolved on ethylene glycol also grow efficiently on 1,4-butanediol (**Figure S5**). Expression *in trans* of the mutated regulator from B10.2 containing this mutation (denoted as PP_2046E) in *P. putida* KT2440 ΔPP_2046 enhanced growth of the wildtype on 1,4-butanediol, while expression of the native version could not restore growth (**Figure 5**). The regulator PP_2046 groups in the LysR-type family, which mainly transcriptional activators, repressors, and even dual function activators/repressors with a helix-turn-helix (HTH) DNA-binding domain at the N-terminus (Pérez-Rueda and Collado-Vides, 2000; Maddocks and Oyston, 2008). Both mutations found in the B10.1 and B10.2 evolved strains are located in the first third of the gene, in the HTH domain. While the B10.1 version of PP_2046 lost its native start codon, alternatives start codons are present (**Figure S1**). The fact that only the mutated version of PP_2046 can enable growth on 1,4-butanediol, while its deletion abolishes growth, strongly suggests that this gene encodes an activator of the downstream operon, with an unknown inducer outside of the 1,4-butanediol context. It seems that a modification of the HTH domain is key to creating a constitutive activator.

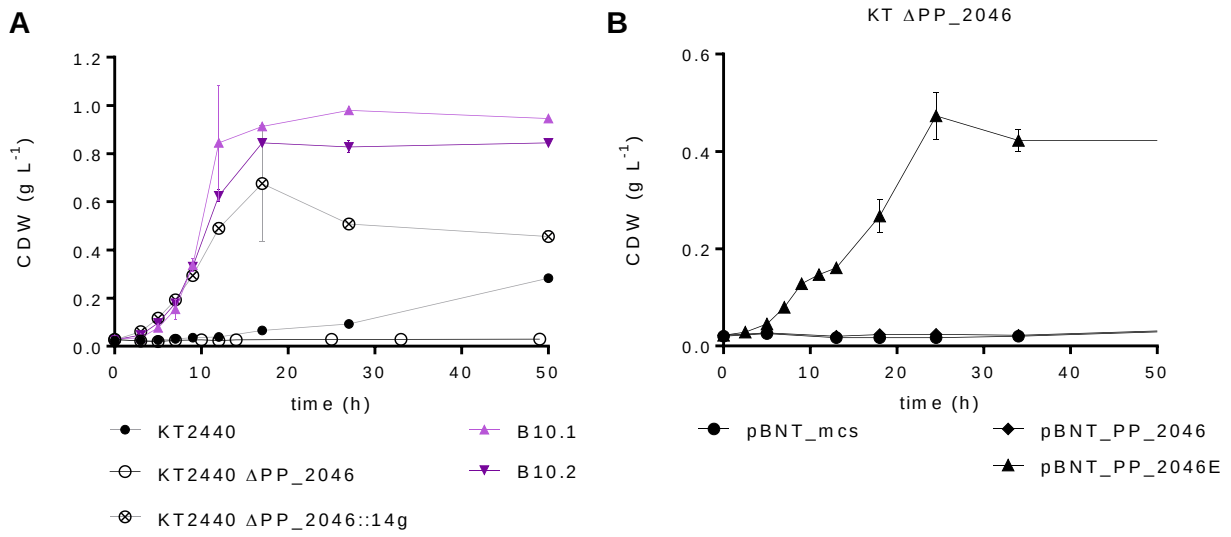

Figure 5 A) Biomass growth during the cultivation of *P. putida* KT2440 (black, circles), B10.1, B10.2 (purple, triangles), *P. putida* KT2440 ΔPP_2046 (black, circle) and *P. putida* KT2440 ΔPP_2046::14g (black, circled cross) in MSM medium with 20 mM 1,4-butanediol. **B**) Biomass growth of *P. putida* KT2440 ΔPP_2046 transformants harboring an overexpressing construct for PP_2046 or PP_2046E and the empty vector cultivated in MSM with 20 mM 1,4-butanediol. Error bars indicate the deviation of the mean (n = 2).

In order to test whether overexpression of the PP_2047-51 operon alone was sufficient to enable faster growth on 1,4-butanediol, PP_2046 was replaced by the strong constitutive promotor P_{14g}, facing the operon, resulting in the strain *P. putida* KT2440 ΔPP_2046::14g. Indeed, the growth on 1,4-butanediol was enhanced by 3.43-fold compared to the wildtype (**Figure 5**). This further indicates that the PP_2047-51 operon is the main determinant enabling fast growth on 1,4-butanediol. However, growth of this strain was somewhat slower than that of the evolved strains (ΔPP_2046::14g: 0.249 ± 0.004 h^{-1}), indicating that other factors, possibly also regulated by PP_2046, are at play.

In this context, it should be noted that no gene encoding a CoA-ligase or transferase is present within the operon, which would be required for 1,4-butanediol degradation through β-oxidation. However, several of such enzymes were upregulated in the presence of 1,4-butanediol (**Figure 3**). To test whether the upregulation of this operon in the evolved strains enables enhanced β-oxidation, growth of the wildtype, the evolved strains, and ΔPP_2046 were analyzed on longer-chain α,ω-diols. The ΔPP_2046 strain did not grow on any of the tested diols. In contrast, both the evolved strain and the wildtype grew on 1,4-butanediol and 1,8-octanediol, with the evolved strains growing at a significantly higher rate (**Figure 6**). Surprisingly, none of the strains grew on 1,6-hexanediol or 1,7-heptanediol. A similar trend of faster growth by the evolved strains was also observed on butanol (**Figure S6**). Since these substrates can only be metabolized through β-oxidation, these results strongly suggest that the upregulation of the PP_2047-51 operon enables higher activity of this pathway, and they prove that PP_2046 is an essential regulator for the metabolism of these short- to medium-chain alcohols.

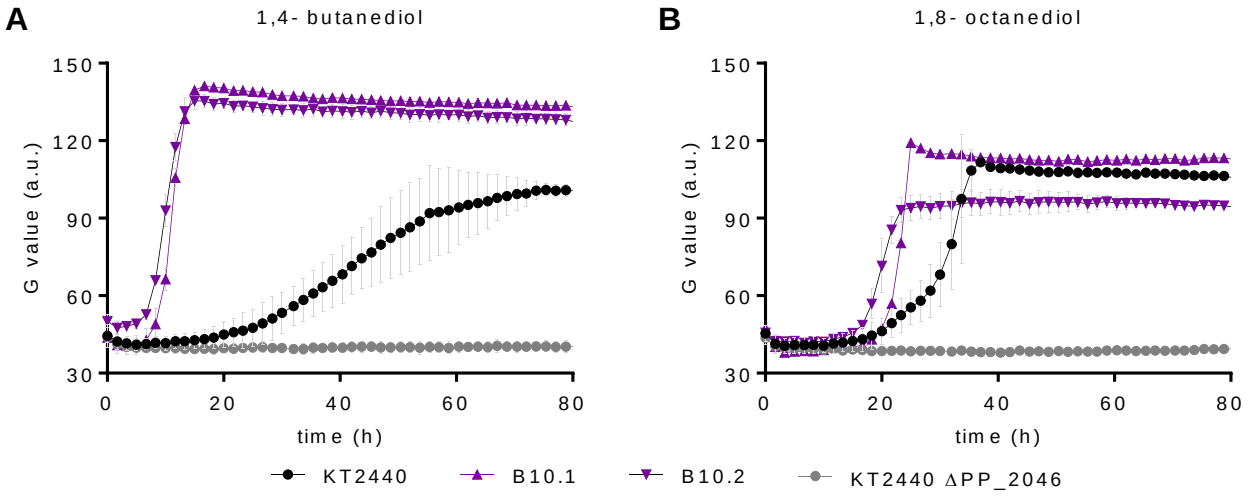

Figure 6 Growth of *P. putida* KT2440 (black, circles), B10.1, B10.2 (purple, triangles) and ΔPP_2046 (grey, circles) on 1,4-butanediol (**A**) and (**B**) 1,8-octanediol. Growth was detected via a Growth Profiler® in 24-square well plates. Error bars depict the deviation from mean (n = 2).

4 Conclusion

Adaptive laboratory evolution was successfully used to enhance growth of *P. putida* KT2440 on 1,4-butanediol. Putative degradation pathways of this important plastic monomer were contextualized with leads from genome resequencing and proteome analysis, which were verified by knockout and overexpression analyses and physiological data. The alcohol dehydrogenases PedE and PP_2049 were found to be essential for growth on 1,4-butanediol, with the latter also being required for growth on 4-hydroxybutyrate. Mutations in the transcriptional regulator PP_2046 were the main cause of enhanced growth in the ALE strains. The evolved phenotype could be reproduced through reverse engineering, either by overexpression of the PP_2047-51 operon by promoter exchange, or through *in trans* expression of the mutated regulator. In all, the knockout analysis favors the hypothesis of direct oxidation of 1,4-butanediol, via 4-hydroxybutyrate, to succinate. However, the alternative β-oxidation hypothesis can't be ruled out, and possibly both pathways operate simultaneously.

5 Author Contributions

NW and LMB conceived the study with the help of KO and TN. NW supervised the study with support of LMB and KO. NW and WJL designed the experiments. WJL performed the experiments with the help of PJN. TN performed the proteome analysis. All authors analyzed and interpreted the data. WJL and NW prepared the figures and wrote the manuscript with the help of all authors. All authors have read and approved the final version of this manuscript.

6 Conflict of Interest

Author Shane T. Kenny was employed by the company Bioplastech Ltd. Author Kevin O'Connor is employed by university college Dublin. He has a shareholding in the company Bioplastech Ltd. The

remaining authors declare that the research was conducted in the absence of any commercial or financial relationships that could be construed as a potential conflict of interest.

7 Funding

The RWTH and UCD researchers acknowledge funding from the European Union´s Horizon 2020 research and innovation programme under grant agreement no. 633962 for the project P4SB and no. 863922 for the project MIX-UP. Nick Wierckx was supported by the German Research Foundation through the Emmy Noether project WI 4255/1-1. The laboratory of Lars M. Blank was partially funded by the Deutsche Forschungsgemeinschaft (DFG, German Research Foundation) under Germany´s excellence strategy within the clusters of excellence 236 "TMFB – Tailor-Made Fuels from Biomass" and 2186 „FSC – The Fuel Science Center". Tanja Narancic and Kevin O'Connor acknowledge the funding form Science foundation Ireland research centre Grant No. SFI/16/RC/3889.

8 Acknowledgments

The authors gratefully acknowledge Janosch Klebensberger (University of Stuttgart), Gregg Beckham (NREL), Jörg Pietruszka (HHU Düsseldorf), as well as all P4SB partners, for helpful discussion.

9 Supplementary Material

Supplemental tables and figures.pdf

Supplemental proteome analysis data.xlsx

10 Data availability statement

The sequences have been deposited in the NCBI Sequence Read Archive (SRA) with the accession number SRP148839 for ethylene glycol ALE strains (including our laboratory wildtype SRX4119395 used in this study) and SRP148839 for the 1,4-butanediol ALE strains. Raw data for all figures shown is available from the author upon reasonable request.

REFERENCES

Bandounas, L., Ballerstedt, H., Winde, J. H. de, and Ruijssenaars, H. J. (2011). Redundancy in putrescine catabolism in solvent tolerant *Pseudomonas putida* S12. *J Biotechnol* 154, 1–10.

Basler, G., Thompson, M., Tullman-Ercek, D., and Keasling, J. (2018). A Pseudomonas putida efflux pump acts on short-chain alcohols. *Biotechnology for biofuels* 11, 136. doi: 10.1186/s13068-018-1133-9

Bednarz, A., Spieß, A. C., and Pfennig, A. (2017). Reactive and physical extraction of bio-based diamines from fermentation media. *J. Chem. Technol. Biotechnol* 92, 1817–1824. doi: 10.1002/jctb.5183

Behrendt, G., and Naber, B. (2009). The chemical recycling of polyurethanes. *J Univ Chem Technol Metallurgy* 44, 3–23.

Belda, E., van Heck, R. G. A., José Lopez-Sanchez, M., Cruveiller, S., Barbe, V., Fraser, C., et al. (2016). The revisited genome of *Pseudomonas putida* KT2440 enlightens its value as a robust metabolic chassis. *Environ Microbiol* 18, 3403–3424. doi: 10.1111/1462-2920.13230

Brandl, H., Gross, R. A., Lenz, R. W., and Fuller, R. C. (1988). *Pseudomonas oleovorans* as a source of poly(beta-hydroxyalkanoates) for potential applications as biodegradable polyesters. *Appl Environ Microb* 54, 1977–1982.

Burgard, A., Burk, M. J., Osterhout, R., van Dien, S., and Yim, H. (2016). Development of a commercial scale process for production of 1,4-butanediol from sugar. *Curr Opin Biotechnol* 42, 118–125. doi: 10.1016/j.copbio.2016.04.016

624 Burger, M., Woods, R. G., McCarthy, C., and Beacham, I. R. (2000). Temperature regulation of protease in
625 *Pseudomonas fluorescens* LS107d2 by an ECF sigma factor and a transmembrane activator. *Microbiology*
626 146 Pt 12, 3149–3155. doi: 10.1099/00221287-146-12-3149
627 Calero, P., Jensen, S. I., Bojanovič, K., Lennen, R. M., Koza, A., and Nielsen, A. T. (2018). Genome-wide
628 identification of tolerance mechanisms toward p-coumaric acid in Pseudomonas putida. *Biotechnology and*
629 *bioengineering* 115, 762–774. doi: 10.1002/bit.26495
630 Chomczynski, P., and Rymaszewski, M. (2006). Alkaline polyethylene glycol-based method for direct PCR
631 from bacteria, eukaryotic tissue samples, and whole blood. *BioTechniques* 40, 454, 456, 458. doi:
632 10.2144/000112149
633 Cox, J., and Mann, M. (2008). MaxQuant enables high peptide identification rates, individualized p.p.b.-range
634 mass accuracies and proteome-wide protein quantification. *Nature biotechnol* 26, 1367–1372. doi:
635 10.1038/nbt.1511
636 Cox, J., Neuhauser, N., Michalski, A., Scheltema, R. A., Olsen, J. V., and Mann, M. (2011). Andromeda: a
637 peptide search engine integrated into the MaxQuant environment. *J Proteome Res* 10, 1794–1805. doi:
638 10.1021/Pr101065j
639 Cuenca, M. d. S., Roca, A., Molina-Santiago, C., Duque, E., Armengaud, J., Gómez-Garcia, M. R., et al.
640 (2016). Understanding butanol tolerance and assimilation in *Pseudomonas putida* BIRD-1: an integrated
641 omics approach. *Microb Biotechnol* 9, 100–115. doi: 10.1111/1751-7915.12328
642 Danso, D., Chow, J., and Streit, W. R. (2019). Plastics: Environmental and Biotechnological Perspectives on
643 Microbial Degradation. *Appl Environ Microb* 85. doi: 10.1128/AEM.01095-19
644 DePristo, M. A., Banks, E., Poplin, R., Garimella, K. V., Maguire, J. R., Hartl, C., et al. (2011). A framework
645 for variation discovery and genotyping using next-generation DNA sequencing data. *Nat Genet* 43, 491–
646 498. doi: 10.1038/ng.806
647 Dragosits, M., and Mattanovich, D. (2013). Adaptive laboratory evolution -- principles and applications for
648 biotechnology. *Microb Cell Fact* 12, 64. doi: 10.1186/1475-2859-12-64
649 Franden, M. A., Jayakody, L. N., Li, W.-J., Wagner, N. J., Cleveland, N. S., Michener, W. E., et al. (2018).
650 Engineering *Pseudomonas putida* KT2440 for efficient ethylene glycol utilization. *Metab Eng* 48, 197–207.
651 doi: 10.1016/j.ymben.2018.06.003
652 Gaona-López, C., Julián-Sánchez, A., and Riveros-Rosas, H. (2016). Diversity and Evolutionary Analysis of
653 Iron-Containing (Type-III) Alcohol Dehydrogenases in Eukaryotes. *PloS one* 11, e0166851. doi:
654 10.1371/journal.pone.0166851
655 Gibson, D. G., Young, L., Chuang, R.-Y., Venter, J. C., Hutchison, C. A., and Smith, H. O. (2009). Enzymatic
656 assembly of DNA molecules up to several hundred kilobases. *Nat Methods* 6, 343–345. doi:
657 10.1038/nmeth.1318
658 Grand View Research (2017). 1,4- butanediol (BDO) Market Report 1,4- butanediol (BDO) Market Analysis
659 By Application (Tetrahydrofuran (THF), Polybutylene Terephthalate (PBT), Gamma-Butyrolactone (GBL),
660 Polyurethane (PU)), By Region (North America, Europe, Asia Pacific, CSA, MEA), And Segment
661 Forecasts, 2018 - 2025. *Grand View Research*.
662 Guzik, M. W., Kenny, S. T., Duane, G. F., Casey, E., Woods, T., Babu, R. P., et al. (2014). Conversion of post
663 consumer polyethylene to the biodegradable polymer polyhydroxyalkanoate. *Appl Microbiol Biot* 98, 4223–
664 4232. doi: 10.1007/s00253-013-5489-2
665 Hanahan, D. (1983). Studies on transformation of *Escherichia coli* with plasmids. *J Mol Biol* 166, 557–580.
666 doi: 10.1016/S0022-2836(83)80284-8
667 Hartmans S., Smiths, J. P., van der Werf, M. J., Volkering, F., and Bont, J.A.M. de (1989). Metabolism of
668 styrene oxide and 2-phenylethanol in the styrene-degrading *Xanthobacter* strain 124X. *Appl Environ*
669 *Microb* 55, 2850–2855.
670 Hiu, S. F., Zhu, C. X., Yan, R. T., and Chen, J. S. (1987). Butanol-Ethanol Dehydrogenase and Butanol-
671 Ethanol-Isopropanol Dehydrogenase: Different Alcohol Dehydrogenases in Two Strains of *Clostridium*
672 *beijerinckii* (*Clostridium butylicum*). *Appl Environ Microb* 53, 697–703.
673 Howard, G. T. (2002). Biodegradation of polyurethane: a review. *Int Biodeterior Biodegradation* 49, 245–252.
674 doi: 10.1016/S0964-8305(02)00051-3

675 Huang, D. W., Sherman, B. T., and Lempicki, R. A. (2009a). Bioinformatics enrichment tools: paths toward
676 the comprehensive functional analysis of large gene lists. *Nucleic Acids Res* 37, 1–13. doi:
677 10.1093/nar/gkn923
678 Huang, D. W., Sherman, B. T., and Lempicki, R. A. (2009b). Systematic and integrative analysis of large gene
679 lists using DAVID bioinformatics resources. *Nat Protoc* 4, 44–57. doi: 10.1038/nprot.2008.211
680 Huerta-Cepas, J., Szklarczyk, D., Forslund, K., Cook, H., Heller, D., Walter, M. C., et al. (2016). eggNOG
681 4.5: a hierarchical orthology framework with improved functional annotations for eukaryotic, prokaryotic
682 and viral sequences. *Nucleic Acids Res* 44, D286-93. doi: 10.1093/nar/gkv1248
683 Hung, C.-S., Zingarelli, S., Nadeau, L. J., Biffinger, J. C., Drake, C. A., Crouch, A. L., et al. (2016). Carbon
684 Catabolite Repression and Impranil Polyurethane Degradation in *Pseudomonas protegens* Strain Pf-5. *Appl*
685 *Environ Microb* 82, 6080–6090. doi: 10.1128/AEM.01448-16
686 Kagi, J. H., and Vallee B. H. (1960). The role of zinc in alcohol dehydrogenase. V. The effect of metal-
687 binding agents on the structure of the yeast alcohol dehydrogenase molecule. *J Biol Chem* 235, 3188–3192.
688 Kenny, S. T., Runic, J. N., Kaminsky, W., Woods, T., Babu, R. P., Keely, C. M., et al. (2008). Up-Cycling of
689 PET (Polyethylene Terephthalate) to the biodegradable plastic PHA (Polyhydroxyalkanoate). *Environ Sci*
690 *Technol* 42, 7696–7701. doi: 10.1021/es801010e
691 Kenny, S. T., Runic, J. N., Kaminsky, W., Woods, T., Babu, R. P., and O'Connor, K. E. (2012). Development
692 of a bioprocess to convert PET derived terephthalic acid and biodiesel derived glycerol to medium chain
693 length polyhydroxyalkanoate. *Appl Microbiol Biot* 95, 623–633. doi: 10.1007/s00253-012-4058-4
694 Klumpp, S., Zhang, Z., and Hwa, T. (2009). Growth rate-dependent global effects on gene expression in
695 bacteria. *Cell* 139, 1366–1375. doi: 10.1016/j.cell.2009.12.001
696 Lageveen, R. G., Huisman, G. W., Preusting, H., Ketelaar, P., Eggink, G., and Witholt, B. (1988). Formation
697 of polyesters by *Pseudomonas oleovorans*: Effect of substrates on formation and composition of poly-(R)-3-
698 hydroxyalkanoates and poly-(R)-3-hydroxyalkenoates. *Appl Environ Microb* 54, 2924–2932.
699 Lennen, R. M., Jensen, K., Mohammed, E. T., Malla, S., Börner, R. A., Chekina, K., et al. (2019). *Adaptive*
700 *laboratory evolution reveals general and specific chemical tolerance mechanisms and enhances*
701 *biochemical production*.
702 Li, H., and Durbin, R. (2009). Fast and accurate short read alignment with Burrows-Wheeler transform.
703 *Bioinformatics* 25, 1754–1760. doi: 10.1093/bioinformatics/btp324
704 Li, W.-J., Jayakody, L. N., Franden, M. A., Wehrmann, M., Daun, T., Hauer, B., et al. (2019). Laboratory
705 evolution reveals the metabolic and regulatory basis of ethylene glycol metabolism by *Pseudomonas putida*
706 KT2440. *Environ Microbiol*. doi: 10.1111/1462-2920.14703
707 Liu, H., and Lu, T. (2015). Autonomous production of 1,4-butanediol via a de novo biosynthesis pathway in
708 engineered *Escherichia coli*. *Metab Eng* 29, 135–141. doi: 10.1016/j.ymben.2015.03.009
709 Maddocks, S. E., and Oyston, P. C. F. (2008). Structure and function of the LysR-type transcriptional
710 regulator (LTTR) family proteins. *Microbiology* 154, 3609–3623. doi: 10.1099/mic.0.2008/022772-0
711 Magnin, A., Hoornaert, L., Pollet, E., Laurichesse, S., Phalip, V., and Avérous, L. (2019a). Isolation and
712 characterization of different promising fungi for biological waste management of polyurethanes. *Microb*
713 *Biotechnol* 12, 544–555. doi: 10.1111/1751-7915.13346
714 Magnin, A., Pollet, E., Perrin, R., Ullmann, C., Persillon, C., Phalip, V., et al. (2019b). Enzymatic recycling of
715 thermoplastic polyurethanes: Synergistic effect of an esterase and an amidase and recovery of building
716 blocks. *Waste Manag* 85, 141–150. doi: 10.1016/j.wasman.2018.12.024
717 Martínez-García, E., Aparicio, T., Lorenzo, V. de, and Nikel, P. I. (2014). New transposon tools tailored for
718 metabolic engineering of gram-negative microbial cell factories. *Front Bioeng Biotechnol* 2, 1–13. doi:
719 10.3389/fbioe.2014.00046
720 Martínez-García, E., and Lorenzo, V. de (2011). Engineering multiple genomic deletions in Gram-negative
721 bacteria: Analysis of the multi-resistant antibiotic profile of *Pseudomonas putida* KT2440. *Environ*
722 *Microbiol* 13, 2702–2716. doi: 10.1111/j.1462-2920.2011.02538.x
723 McKenna, A., Hanna, M., Banks, E., Sivachenko, A., Cibulskis, K., Kernytsky, A., et al. (2010). The genome
724 analysis toolkit: A MapReduce framework for analyzing next-generation DNA sequencing data. *Genome*
725 *Res* 20, 1297–1303. doi: 10.1101/gr.107524.110

Mitchell, A. L., Attwood, T. K., Babbitt, P. C., Blum, M., Bork, P., Bridge, A., et al. (2019). InterPro in 2019: improving coverage, classification and access to protein sequence annotations. *Nucleic acids research* 47, D351-D360. doi: 10.1093/nar/gky1100

Narancic, T., and O'Connor, K. E. (2017). Microbial biotechnology addressing the plastic waste disaster. *Microb Biotechnol* 10, 1232–1235. doi: 10.1111/1751-7915.12775

Narancic, T., Scollica, E., Kenny, S. T., Gibbons, H., Carr, E., Brennan, L., et al. (2016). Understanding the physiological roles of polyhydroxybutyrate (PHB) in *Rhodospirillum rubrum* S1 under aerobic chemoheterotrophic conditions. *Appl Microbiol Biotechnol* 100, 8901–8912. doi: 10.1007/s00253-016-7711-5

Nelson, K. E., Weinel, C., Paulsen, I. T., Dodson, R. J., Hilbert, H., Martins dos Santos, V A P, et al. (2002). Complete genome sequence and comparative analysis of the metabolically versatile *Pseudomonas putida* KT2440. *Environ Microbiol* 4, 799–808.

Nikel, P. I., and Lorenzo, V. de (2018). *Pseudomonas putida* as a functional chassis for industrial biocatalysis: From native biochemistry to trans-metabolism. *Metab Eng* 50, 142–155. doi: 10.1016/j.ymben.2018.05.005

Nikel, P. I., Martínez-García, E., and Lorenzo, V. de (2014). Biotechnological domestication of Pseudomonads using synthetic biology. *Nat Rev Microbiol* 12, 368–379. doi: 10.1038/nrmicro3253

Noel, J. K., and Whitford, P. C. (2016). How EF-Tu can contribute to efficient proofreading of aa-tRNA by the ribosome. *Nat Commun* 7, 13314 EP. doi: 10.1038/ncomms13314

Parke, D., Garcia, M. A., and Ornston, L. N. (2001). Cloning and Genetic Characterization of dca Genes Required for -Oxidation of Straight-Chain Dicarboxylic Acids in *Acinetobacter sp*. Strain ADP1. *Appl Environ Microb* 67, 4817–4827. doi: 10.1128/AEM.67.10.4817-4827.2001

Pérez-Rueda, E., and Collado-Vides, J. (2000). The repertoire of DNA-binding transcriptional regulators in Escherichia coli K-12. *Nucleic Acids Res* 28, 1838–1847. doi: 10.1093/nar/28.8.1838

Poblete-Castro, I., Escapa, I. F., Jäger, C., Puchalka, J., Lam, C. M. C., Schomburg, D., et al. (2012). The metabolic response of *P. putida* KT2442 producing high levels of polyhydroxyalkanoate under single- and multiple-nutrient-limited growth: highlights from a multi-level omics approach. *Microb Cell Fact* 11, 34. doi: 10.1186/1475-2859-11-34.

Ramos, J. L., Duque, E., Gallegos, M.-T., Godoy, P., Ramos-Gonzalez, M. I., Rojas, A., et al. (2002). Mechanisms of solvent tolerance in gram-negative bacteria. *Annu Rev Microbiol* 56, 743–768. doi: 10.1146/annurev.micro.56.012302.161038

Rühl, J., Schmid, A., and Blank, L. M. (2009). Selected *Pseudomonas putida* strains able to grow in the presence of high butanol concentrations. *Appl Environ Microb* 75, 4653–4656. doi: 10.1128/AEM.00225-09

Samanta, S. K., Singh, O. V., and Jain, R. K. (2002). Polycyclic aromatic hydrocarbons: environmental pollution and bioremediation. *Trends Biotechnol* 20, 243–248. doi: 10.1016/S0167-7799(02)01943-1

Schmidt, J., Wei, R., Oeser, T., Dedavid E Silva, L. A., Breite, D., Schulze, A., et al. (2017). Degradation of Polyester Polyurethane by Bacterial Polyester Hydrolases. *Polymers* 9. doi: 10.3390/polym9020065

Simon, O., Klebensberger, J., Mükschel, B., Klaiber, I., Graf, N., Altenbuchner, J., et al. (2015). Analysis of the molecular response of *Pseudomonas putida* KT2440 to the next-generation biofuel n-butanol. *J Proteom* 122, 11–25. doi: 10.1016/j.jprot.2015.03.022

Spini, G., Spina, F., Poli, A., Blieux, A.-L., Regnier, T., Gramellini, C., et al. (2018). Molecular and Microbiological Insights on the Enrichment Procedures for the Isolation of Petroleum Degrading Bacteria and Fungi. *Front Microbiol* 9. doi: 10.3389/fmicb.2018.02543

Steele, M. I., Lorenz, D., Hatter, K., Park, A., and Sokatch, J. R. (1992). Characterization of the *mmsAB* operon of *Pseudomonas aeruginosa* PAO encoding methylmalonate-semialdehyde dehydrogenase and 3-hydroxyisobutyrate dehydrogenase. *J Biol Chem* 267, 13585–13592.

Tahseen, R., Arslan, M., Iqbal, S., Khalid, Z. M., and Afzal, M. (2019). Enhanced degradation of hydrocarbons by gamma ray induced mutant strain of *Pseudomonas putida*. *Biotechnol Lett* 41, 391–399. doi: 10.1007/s10529-019-02644-y

Takeda, K., Matsumura, H., Ishida, T., Samejima, M., Igarashi, K., Nakamura, N., et al. (2013). The two-step electrochemical oxidation of alcohols using a novel recombinant PQQ alcohol dehydrogenase as a catalyst for a bioanode. *Bioelectrochemistry* 94, 75–78. doi: 10.1016/j.bioelechem.2013.08.001

Tatusov, R. L., Koonin, E. V., and Lipman, D. J. (1997). A genomic perspective on protein families. *Science* 278, 631–637. doi: 10.1126/science.278.5338.631

779 The UniProt Consortium (2019). UniProt: a worldwide hub of protein knowledge. *Nucleic Acids Res* 47,
780 D506-D515. doi: 10.1093/nar/gky1049
781 Thorvaldsdóttir, H., Robinson, J. T., and Mesirov, J. P. (2013). Integrative Genomics Viewer (IGV): High-
782 performance genomics data visualization and exploration. *Brief Bioinform* 14, 178–192. doi:
783 10.1093/bib/bbs017
784 Tyanova, S., Temu, T., Sinitcyn, P., Carlson, A., Hein, M. Y., Geiger, T., et al. (2016a). The perseus
785 computational platform for comprehensive analysis of (prote)omics data. *Nat Methods* 13, 731–740. doi:
786 10.1038/nmeth.3901
787 Tyanova, S., Temu, T., Sinitcyn, P., Carlson, A., Hein, M. Y., Geiger, T., et al. (2016b). The Perseus
788 computational platform for comprehensive analysis of (prote)omics data. *Nat Methods* 13, 731–740. doi:
789 10.1038/nmeth.3901
790 Vallon, T., Simon, O., Rendgen-Heugle, B., Frana, S., Mückschel, B., Broicher, A., et al. (2015). Applying
791 systems biology tools to study *n*-butanol degradation in *Pseudomonas putida* KT2440. *Eng Life Sci* 15,
792 760–771.
793 Wang, J. C. (2002). Cellular roles of DNA topoisomerases: a molecular perspective. *Nat Rev Mol Cell Biol* 3,
794 430–440. doi: 10.1038/nrm831
795 Wang, W., Zhou, H., Lin, H., Roy, S., Shaler, T. A., Hill, L. R., et al. (2003). Quantification of Proteins and
796 Metabolites by Mass Spectrometry without Isotopic Labeling or Spiked Standards. *Anal Chem* 75, 4818–
797 4826. doi: 10.1021/Ac026468x
798 Ward, P. G., Goff, M., Donner, M., Kaminsky, W., and O'Connor, K. E. (2006). A two step chemo-
799 biotechnological conversion of polystyrene to a biodegradable thermoplastic. *Environ Sci Technol* 40,
800 2433–2437. doi: 10.1021/es0517668
801 Wehrmann, M., Billard, P., Martin-Meriadec, A., Zegeye, A., and Klebensberger, J. (2017). Functional Role
802 of Lanthanides in Enzymatic Activity and Transcriptional Regulation of Pyrroloquinoline Quinone-
803 Dependent Alcohol Dehydrogenases in *Pseudomonas putida* KT2440. *mBio* 8. doi: 10.1128/mBio.00570-17
804 Wierckx, N., Koopman, F., Ruijssenaars, H. J., and Winde, J. H. de (2011). Microbial degradation of furanic
805 compounds: biochemistry, genetics, and impact. *Appl Microbiol Biotechnol* 92, 1095–1105. doi:
806 10.1007/s00253-011-3632-5
807 Wierckx, N., Prieto, M. A., Pomposiello, P., Lorenzo, V. de, O'Connor, K., and Blank, L. M. (2015). Plastic
808 waste as a novel substrate for industrial biotechnology. *Microb Biotechnol* 8, 900–903. doi: 10.1111/1751-
809 7915.12312
810 Wilkes, R.A., and Aristilde, L. (2017) Degradation and metabolism of synthetic plastics and associated
811 products by *Pseudomonas* sp. capabilities and challenges. *J Appl Microbiol* 123, 582–593.
812 Wynands, B., Lenzen, C., Otto, M., Koch, F., Blank, L. M., and Wierckx, N. (2018). Metabolic engineering of
813 *Pseudomonas taiwanensis* VLB120 with minimal genomic modifications for high-yield phenol production.
814 *Metab Eng* 47, 121–133. doi: 10.1016/j.ymben.2018.03.011
815 Yim, H., Haselbeck, R., Niu, W., Pujol-Baxley, C., Burgard, A., Boldt, J., et al. (2011). Metabolic engineering
816 of *Escherichia coli* for direct production of 1,4-butanediol. *Nat Chem Biol* 7, 445–452. doi:
817 10.1038/nchembio.580
818 Zhou, S., Mohan Raj, S., Ashok, S., Edwardraja, S., Lee, S.-G., and Park, S. (2013). Cloning, expression and
819 characterization of 3-hydroxyisobutyrate dehydrogenase from *Pseudomonas denitrificans* ATCC 13867.
820 *PloS one* 8, e62666.
821 Zia, K. M., Bhatti, H. N., and Ahmad Bhatti, I. (2007). Methods for polyurethane and polyurethane
822 composites, recycling and recovery: A review. *Reactive and Functional Polymers* 67, 675–692. doi:
823 10.1016/j.reactfunctpolym.2007.05.004

Supplemental data to:

Unraveling 1,4-butanediol metabolism in *Pseudomonas putida* KT2440

Wing-Jin Li[1], Tanja Narancic[2,3], Shane T. Kenny[4], Paul-Joachim Niehoff[1], Kevin O'Connor[2,3], Lars M. Blank[1], Nick Wierckx[1,5]*

[1] Institute of Applied Microbiology-iAMB, Aachen Biology and Biotechnology-ABBt, RWTH Aachen University, Aachen, Germany

[2] UCD Earth Institute and School of Biomolecular and Biomedical Science, University College Dublin, Belfield, Dublin 4, Ireland

[3] BEACON – SFI Bioeconomy Research Centre, University College Dublin, Belfield, Dublin 4, Ireland

[4] Bioplastech Ltd., NovaUCD, Belfield Innovation Park, University College Dublin, Belfield, Dublin 4, Ireland

[5] Institute of Bio- and Geosciences IBG-1: Biotechnology, Forschungszentrum Jülich, 52425 Jülich, Germany

*** Correspondence:** n.wierckx@fz-juelich.de

Table S1 Oligonucleotides used in this work

name	sequence	template	direc-tion	purpose
MO48	ACTATAGGGCGAATTGGAGC	*P. putida* KT2440	rw	pBNT
WJ49	GCTCGGTACCCGGGGATCCTCTAGAGAATTCAGTACTGGTGGCCGAAGA	*P. putida* KT2440	fw	pEMG_ΔPP_0411
WJ50	GCAAGGATCCCCTAGGGGGGGTACTGAGAGAATG	*P. putida* KT2440	rw	pEMG_ΔPP_0411
WJ51	CAGTACCCCCCCTAGGGGATCCTTGCCTGTACCGGCCTCTTC	*P. putida* KT2440	fw	pEMG_ΔPP_0411
WJ52	TGCATGCCTGCAGGTCGACTCTAGAGTCGACCAGCGTCCCCGGGAACAG	*P. putida* KT2440	rw	pEMG_ΔPP_0411
WJ54	AGATTGAGCTGGTACGTGAG	*P. putida* KT2440	fw	pEMG_ΔPP_0411
WJ55	GCATAAGCGTCCATGAACAG	*P. putida* KT2440	rw	pEMG_ΔPP_0411
M13uni (-43)	AGGGTTTTCCCAGTCACGACGTT	pEMG	fw	pEMG
M13rev (-49)	GAGCGGATAACAATTTCACACAGG	pEMG	rw	pEMG
WJ56	TCTCGGTACCCGCTGGCCCTTAACATTCCC	*P. putida* KT2440	fw	pEMG_Δ*pedE*
WJ57	CCGCTCTAGAAATTTCCACCCGCTATTCAC	*P. putida* KT2440	rw	pEMG_Δ*pedE*
WJ58	TACATCTAGACACCTCAATTGGCCCTTCGC	*P. putida* KT2440	fw	pEMG_Δ*pedE*
WJ59	ATTCGTCGACTTGTACACCGCCACCTTGAG	*P. putida* KT2440	rw	pEMG_Δ*pedE*
WJ60	TCTCGAGCTCCTCACCGACAAGCCGGTAG	*P. putida* KT2440	fw	pEMG_Δ*pedH*
WJ61	TCTCGGATCCTCTTGGTCCCGACCCGATTG	*P. putida* KT2440	rw	pEMG_Δ*pedH*
WJ62	TCTCGGATCCCGGCCCTACTACCAAATGAC	*P. putida* KT2440	fw	pEMG_Δ*pedH*
WJ63	TCTCGTCGACTCTTGGCAATGCGCTTGCTG	*P. putida* KT2440	rw	pEMG_Δ*pedH*
WJ64	TCTCGGTACCACGTGCTCGACCGCACCAAC	*P. putida* KT2440	fw	pEMG_Δ*pedI*
WJ65	ATCGTCTAGATTTGGTAGTAGGGCCGCTTG	*P. putida* KT2440	rw	pEMG_Δ*pedI*
WJ66	ATCGTCTAGAGCCCGCTCCCACAGGTTCAC	*P. putida* KT2440	fw	pEMG_Δ*pedI*
WJ67	ATCGGTCGACGGCACCAAAGATGATTTCAG	*P. putida* KT2440	rw	pEMG_Δ*pedI*
WJ68	GGGCTTGCGCCTGTTCATTC	*P. putida* KT2440	fw	sequencing *pedE*
WJ69	GCTGTGTACAGGCAGTAGTC	*P. putida* KT2440	rw	sequencing *pedI*
WJ74	TCTCGAATTCTCCGGCATCCACCTGGCCTC	*P. putida* KT2440	fw	pEMG_ΔPP_2046
WJ75	TCTCGGTACCAGCCATCAGGAAACGCGATAG	*P. putida* KT2440	rw	pEMG_ΔPP_2046

name	sequence	template	direc-tion	purpose
WJ76	TCTCGGTACCTACCTTCGGCCTGCTTAGGG	*P. putida* KT2440	fw	pEMG_ΔPP_2046
WJ77	TTCCTCTAGATCCAGGTCGATGCCCACCAC	*P. putida* KT2440	rw	pEMG_ΔPP_2046
WJ80	TGAGGCTGACAGTGGCATTG	*P. putida* KT2440	fw	sequencing PP_2046
WJ81	AGCGCATTATCGACCTGCAC	*P. putida* KT2440	rw	sequencing PP_2046
WJ93	AGGTACCGAATTCCTCGAGTTAGGAGGTATTTCGTATGCCATATATTTTC AGCATGAATATTTCGAACTTCGACCTGAACCTG	*P. putida* KT2440 E12 evo1	fw	pBNT_PP_2046E
WJ94	GCCCGACGTCGCATGCTCCTTCTAGATCAGGCGGGGGGGAGCGT	*P. putida* KT2440 E12 evo1	rw	pBNT_PP_2046E
WJ95	ACGCTCCTGCTTTCTTGTAG	*P. putida* KT2440	rw	sequencing PP_2046
WJ96	GAATAGCGGGTGGAAATTGG	*P. putida* KT2440	fw	sequencing *pedE*
WJ102	TTCCGAATTCTGCATGCCCTGGCCTATCCG	*P. putida* KT2440	fw	pEMG_ΔPP_2051
WJ103	TTCCAGGTACCCTTTCATGATGGCTGTTCC	*P. putida* KT2440	rw	pEMG_ΔPP_2051
WJ104	TTCCGGTACCCAAGGCCAGCCCATGGCGCTGAC	*P. putida* KT2440	fw	pEMG_ΔPP_2051
WJ105	TTCCTCTAGACAGCAGCGCCATGAGCCAGC	*P. putida* KT2440	rw	pEMG_ΔPP_2051
WJ106	GCTGCTGGCGGATAACCTTG	*P. putida* KT2440	fw	mapping PP_2051
WJ107	GCACACGCAAATCTTCAACG	*P. putida* KT2440	rw	mapping PP_2051
WJ119	AGCTCGGTACCCGGGGATCCTCCGGCATCCACCTGGCCTC	*P. putida* KT2440	fw	pEMG_ΔPP_2046::14g
WJ120	CCTAGGTCGTGCAATTATACCTGGCCGCGAGAGCCTTGTCAATGGGCTT AATTAAAGCCATCAGGAAACGCGATAG	*P. putida* KT2440	rw	pEMG_ΔPP_2046::14g
WJ121	TTAATTAAGCCCATTGACAAGGCTCTCGCGGCCAGGTATAATTGCACGA CCTAGGTACCTTCGGCCTGCTTAGGG	*P. putida* KT2440	fw	pEMG_ΔPP_2046::14g
WJ122	TGCATGCCTGCAGGTCGACTTCCAGGTCGATGCCCACCAC	*P. putida* KT2440	rw	pEMG_ΔPP_2046::14g
WJ129	GCTCGGTACCCGGGGATCCTGATCCGATCATCGTCCATC	*P. putida* KT2440	fw	pEMG_ΔPP_2049
WJ130	CCTCATAGATCGCACTCTCCTTGTTCGTG	*P. putida* KT2440	rw	pEMG_ΔPP_2049
WJ131	GGAGAGTGCGATCTATGAGGCAGCCTACTGATG	*P. putida* KT2440	fw	pEMG_ΔPP_2049
WJ132	TGCATGCCTGCAGGTCGACTTCCTGACCTGCGCCAATG	*P. putida* KT2440	rw	pEMG_ΔPP_2049
WJ134	GATCGAATTCCCAGATGTGCCGCAAGCCCAG	*P. putida* KT2440	fw	pEMG_ΔPP_2047
WJ135	GTATGGTACCTCCAGCCACAGCACCGACAG	*P. putida* KT2440	rw	pEMG_ΔPP_2047
BW13	TTTGCACTGCCGGTAGAAC	pEMG	fw	pEMG MCS mapping

name	sequence	template	direc-tion	purpose
BW14	AATACGCAAACCGCCTCTC	pEMG	rw	pEMG MCS mapping

Table S2 Plasmids used in this work

plasmid	genotype	reference
pRK2013	Km^r, oriV(RK2/ColE1), mob^+, tra^+	Figurski and Helinski, 1979
pSW-2	Gm^r, oriRK2, xylS, Pm→I-sceI (transcriptional fusion of I-*sceI* to Pm)	Martínez-García and Lorenzo, 2011
pEMG and derivatives		
pEMG	Kan^r, oriR6K, lacZ α wth two flanking I-SceI sites	Martínez-García and Lorenzo, 2011
pEMG_Δ*gcl*	pEMG bearing flanking sequences of *gcl*, *gcl* deletion delivery vector	this work
pEMG_Δ*gclR*	pEMG bearing flanking sequences of ***gclR***, ***gclR*** deletion delivery vector	this work
pEMG_Δ*pedE*	pEMG bearing flanking sequences of *pedE*, *pedE* deletion delivery vector	Li et al., 2019
pEMG_*ΔpedE-I*	pEMG bearing flanking sequences of *pedE-I*, *pedE-I* deletion delivery vector	Li et al., 2019
pEMG_Δ*pedH*	pEMG bearing flanking sequences of *pedH*, *pedH* deletion delivery vector	Li et al., 2019
pEMG_*ΔpedI*	pEMG bearing flanking sequences of *pedI*, *pedI* deletion delivery vector	Li et al., 2019
pEMG_ΔPP_0411-0413	pEMG bearing flanking sequences of PP_0411-13, PP_0411-13 deletion delivery vector	this work
pEMG_ΔPP_2046	pEMG bearing flanking sequences of PP_2046, PP_2046 deletion delivery vector	this work
pEMG_ΔPP_2046::14g	pEMG bearing flanking sequences of PP_2046 and integration of the synthetic promotor 14g, replacing PP_2046 with 14g delivery vector	this work
pEMG_ΔPP_2047-51	pEMG bearing flanking sequences of PP_2047-51, PP_2047-51 deletion delivery vector	this work
pEMG_ΔPP_2049	pEMG bearing flanking sequences of PP_2049, PP_2049 deletion delivery vector	Niehoff (2017)
pEMG_ΔPP_2051	pEMG bearing flanking sequences of PP_2051, PP_2051 deletion delivery vector	this work

plasmid	genotype	reference
pEMG_ΔPP_2662	pEMG bearing flanking sequences of PP_2662, PP_2662 deletion delivery vector	this work
pEMG_ΔPP_2662::14d	pEMG bearing flanking sequences of PP_2662 and integration of the synthetic promotor 14d, replacing PP_2662 with 14d delivery vector	this work
Expression vectors		
pBNT and derivatives		
pBNT	Km^r, P_{nagAa}: nag promoter without RBS, salicylate-inducible	Verhoef et al., 2010
pBNT_PP_2046	pBNT_(MCS) plasmid with PP_2046 from *P. putida* KT2440	this work
pBNT_PP_2046E	pBNT_(MCS) plasmid with evolved PP_2046 from *P. putida* KT2440, E6.1	this work

Table S3 List of mutations (Single Nucleotide Polymorphisms (SNP) and Insertion-Deletion polymorphisms (InDel)) found in the genome of the evolved strains B10.1 (not underlined) or B10.2 (underlined) but not in our laboratory *P. putida* KT2440. The mutated gene found in both evolved strains, but not in the wildtype, is highlighted in bold.

type	strain	position	locus tag	codon change	functional class	annotation
SNP	B10.2	196495	PP_0168	acG/acC	silent	surface adhesion protein
	B10.1	197524	PP_0168	gtA/gtG	silent	
	B10.1	197551	PP_0168	acC/acG	silent	
	B10.2	197551	PP_0168	acC/acG	silent	
	B10.1	197572	PP_0168	aaG/aaA	silent	
	B10.2	197572	PP_0168	aaG/aaA	silent	
	B10.1	197590	PP_0168	gaT/gaC	silent	
	B10.2	197590	PP_0168	gaT/gaC	silent	
	B10.2	698939	PP_16SD	NA	none	rRNA
	B10.2	**2328228**	**PP_2046**	**gAg/gGg**	**missense**	**lysR family regulator**
	B10.1	**2328326**	**PP_2046**	**atG/atA**	**nonsense**	**lysR family regulator**
	B10.2	3287225	PP_2889	gCg/gGg	missense	transmembrane anti-sigma factor
	B10.1	4345003	PP_3818	gaA/gaG	silent	OmpA/ MotB domain-containing protein
	B10.2	4348955	intergenic	NA	none	

type	strain	position	locus tag	codon change	functional class	annotation
InDel	B10.1	2443249	PP_2139	GTGCGCC GCTGGTG CTGGAGA TTGTGCC GCACAAG CATGAGA TCGACCC GAAGTAC CACTTCC TGTGCGA --> G	none	DNA topoisomerase I - topA

ATA→Start loss

TTTTTGAAATTTCCATTTCGTATGCCATATATTTTCAGCATGAATATTTCGAACTTCGACCT
GAACCT GGG→E34G
GCTGCGCGTCTTCGACATGTTGCTGCGTGAACAGAATGTATCCCGGGCAGCCGCGCGTCTGG
CCCTGACCCAGCCGACCGTGAGCAATGCCCTGGCGCGCCTGCGTGACCAGCTGGGTGACCCG
CTGCTGGTCCGCGTGGGCCGGCGCATGCGCCCGACGCCACGGGCCTTGGCACTGGAGGGGCC
GATACGTGCGGCGTTACAGCAGATCGAGCAGACGCTGGGCACCGGCGATGGTTTCGAGCCTC
AGCGCAGCCATCGCCAGCTGCGCATCGCCCTCACCGATTTCGTCGAACAGCTGTGCATGCCG
CCACTCCTGGCGCGGCTGGAGCTACTGGCACCCAACGTGCGCATCGACGTGGTGCACCTGGC
CCCCAACCTGCCGGCCGAGGCGCTGGACCGGGGCGACCTCGACCTGGTACTGGGCCGTTTCG
ACGAGGTGCCGGCGCGCTTCACCCGCCACCCCTGGCGCCGTGAAACCCTGCAGATCGCGCTG
CGCCAGCAGCACCCGCACCTGGCGCCGGGCCAGGCACTGGACCTCGACGCATTCCTGGGCTT
GCGGCACATCTGGGTGCACGGCGGCCAGACCCGGGGCATGGTCGACCAGTGGCTGGCCGAGC
AAGGCCTGACCCGGCAAATCGCCTATACCACGCCCAACTACCTGCAGGCCGCCCATCTGGCC
GCAGCCACCGACATGTGTGTGGTGCTGCCGCGGCAACTGGCGCAGCAGTTTGCGCACCTGCT
GCCATTGGCGGTGCACGAACTGCCATTTGCCCTGGAGCCTTTCGAATTGGAAGTGGTGCACC
TGAGCCACCGTCAGCACGACCCCGCCCTGGCCTGGCTGGTCGAACAGATCCTCACGCTCCCC
CCCGCCTGAAGCCATCAGGAAACGCGATA

Figure S1 Sequence of PP_2046 from *P. putida* KT2440. Native (red) and alternative in-frame (orange) start codons, as well as the mutations in B10.1 (ATG → ATA: start loss) and B10.2 (GCG – GGG: E34G) (blue) are shown. The underlined sequence encodes a putative helix-turn-helix DNA binding domain (Letunic and Bork, 2018).

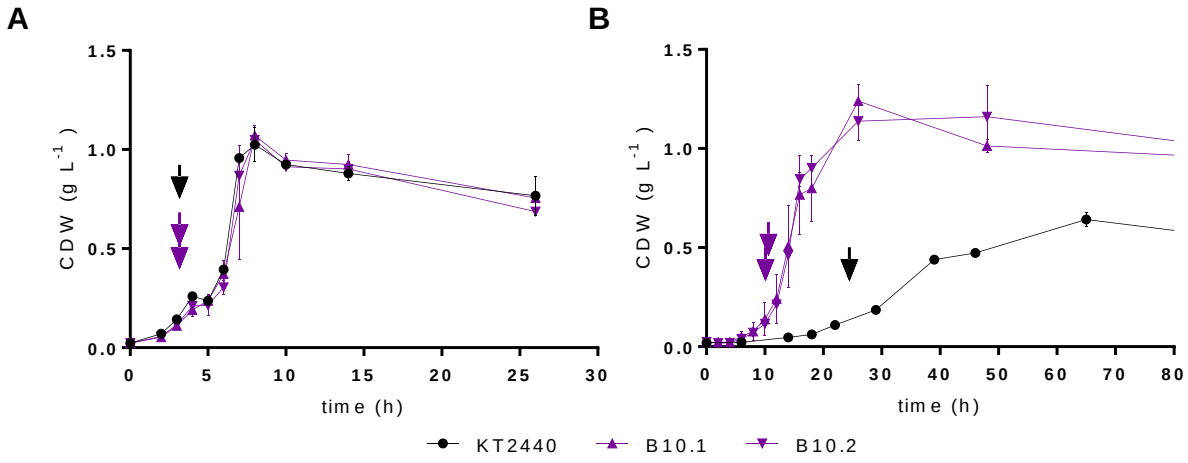

Figure S2 Biomass growth of *P. putida* KT2440 and the evolved strains B10.1 and B10.2 cultivated in MSM with 13.3 mM glucose (**A**) or 20 mM 1,4-butanediol (**B**). Arrows indicate the time when samples were taken for proteome analysis. Error bars indicate the standard deviation (n = 3).

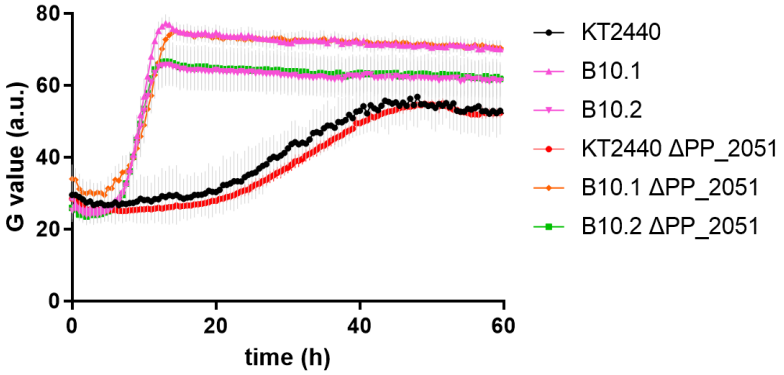

Figure S3 Growth of *P. putida* KT2440 (black, circles), B10.1, B10.2 (purple, triangles) and the respective ΔPP_2051 knockouts in KT2440 (red, circles), B10.1 (orange, diamonds) and B10.2 (green, squares) in MSM with 20 mM 1,4-butanediol. Growth was detected via a Growth Profiler® in 24-square well plates. Error bars depict the standard error of the mean (n = 3).

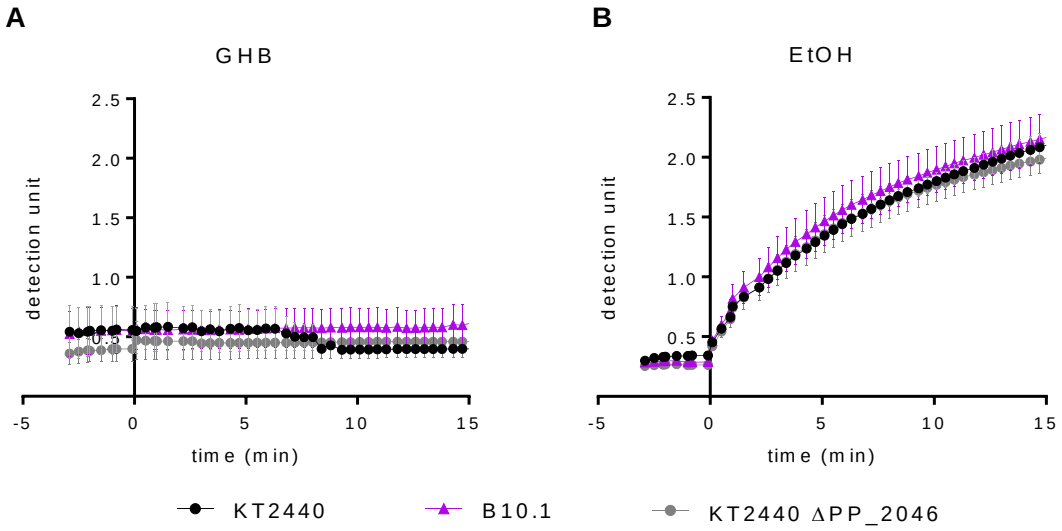

Figure S4 Dehydrogenase activity assay with 4-hydroxybutyrate (GHB) (**A**) or ethanol (EtOH) (**B**) as substrate. Crude cell extracts obtained from *P. putida* KT2440 (black, circles), B10.1, B10.2 (purple, triangles) and *P. putida* KT2440 ΔPP_2046 (grey, circles) Error bars depict the standard error of the mean (n = 2-3).

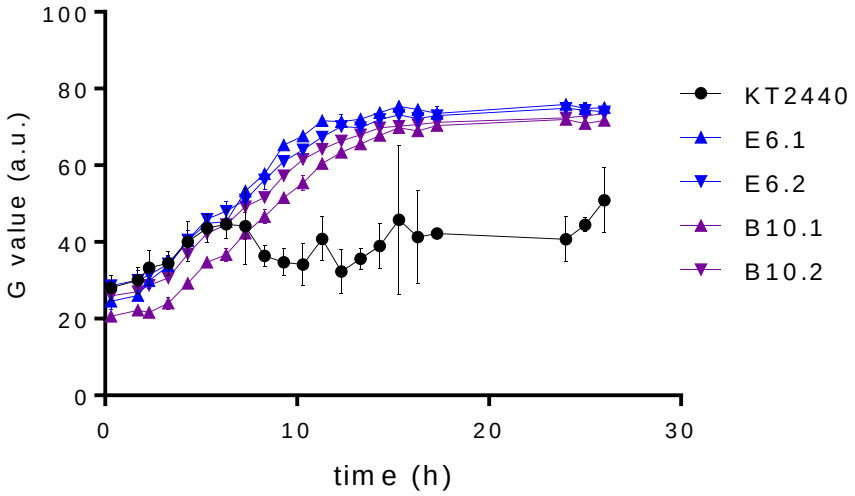

Figure S5 Growth comparison of wildtype *P. putida* KT2440, strains E6.1 and E6.2 evolved on ethylene glycol (Li et al., 2019), and the strains B10.1 and B10.2 evolved on 1,4-butanediol, cultivated in MSM with 20 mM 1,4-butanediol. Growth was detected via the Growth Profiler® in a 24-well plate. Error bars indicate the standard deviation (n=3).

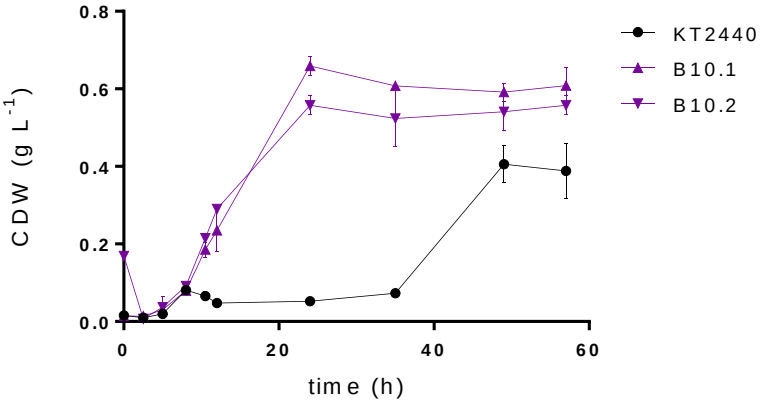

Figure S6 Biomass growth of *P. putida* KT2440 (black, circles) and the evolved strains B10.1 (purple, triangle) and B10.2 (purple, inverted triangle) in shake flasks in MSM with 20 mM 1-butanol. Error bars indicate the deviation of the mean (n = 2).

REFERENCES

Figurski, D. H., and Helinski, D. R. (1979). Replication of an origin-containing derivative of plasmid RK2 dependent on a plasmid function provided in trans. *Pro Natl Acad Sci USA* 76, 1648–1652. doi: 10.1073/pnas.76.4.1648

Letunic, I., and Bork, P. (2018). 20 years of the SMART protein domain annotation resource. *Nucleic acids research* 46, D493-D496. doi: 10.1093/nar/gkx922

Li, W.-J., Jayakody, L. N., Franden, M. A., Wehrmann, M., Daun, T., Hauer, B., et al. (2019). Laboratory evolution reveals the metabolic and regulatory basis of ethylene glycol metabolism by *Pseudomonas putida* KT2440. *Environ Microbiol*. doi: 10.1111/1462-2920.14703

Martínez-García, E., and Lorenzo, V. de (2011). Engineering multiple genomic deletions in Gram-negative bacteria: Analysis of the multi-resistant antibiotic profile of *Pseudomonas putida* KT2440. *Environ Microbiol* 13, 2702–2716. doi: 10.1111/j.1462-2920.2011.02538.x

Verhoef, S., Ballerstedt, H., Volkers, R. J. M., Winde, J. H. de, and Ruijssenaars, H. J. (2010). Comparative transcriptomics and proteomics of p-hydroxybenzoate producing *Pseudomonas putida* S12: novel responses and implications for strain improvement. *Appl Microbiol Biotechnol* 87, 679–690. doi: 10.1007/s00253-010-2626-z